Lessons Learned in Tuning the Optoelectronic Properties of Phosphorescent Iridium(III) Complexes

Adam F. Henwood[a], *Eli Zysman-Colman*[a]*

[a] Organic Semiconductor Centre, EaStCHEM School of Chemistry, University of St Andrews, St Andrews, Fife, KY16 9ST, UK, Fax: +44-1334 463808; Tel: +44-1334 463826; E-mail: eli.zysman-colman@st-andrews.ac.uk;
URL: http://www.zysman-colman.com

Abstract. This perspective illustrates our approach in the design of heteroleptic cationic iridium(III) complexes for optoelectronic applications, especially as emitters in electroluminescent devices. We discuss changes in the photophysical properties of the complexes as a consequence of modification of the electronics of either the cyclometalating (C^N) or the ancillary (N^N) ligands. We then broach the impact on these properties as a function of modification of the structure of both types of ligands. We explain trends in the optoelectronic behaviour of the complexes using a combination of rationally designed structure-property relationship studies and theoretical modelling that serves to inform subsequent ligand design. However, we have found cases where the design paradigms do not always hold true. Nevertheless, all these studies contribute to the lessons we have learned in the design of heteroleptic cationic phosphorescent iridium(III) complexes.

1: Introduction. The efficient phosphorescence exhibited by cyclometalated iridium(III) complexes has made them among the most widely explored classes of transition metal complexes for photonic and optoelectronic applications[1] (behind polypyridyl ruthenium(II) complexes), with applications in everything from sensing[2] and bioimaging[3] to photoredox catalysts for organic transformations[4] and as solar fuels.[5] In our lab, we have a particular interest in utilising complexes of the form $[Ir(C^N)_2(N^N)]PF_6$, where C^N is a cyclomatalating ligand and N^N is an ancillary diimine ligand, as materials for solid-state lighting (SSL) technologies, where it has been shown that these can act as effective phosphors for generating light in electroluminescent devices such as organic light emitting devices (OLEDs)[6] and light-emitting electrochemical cells (LEECs).[7]

An important feature of these complexes, particularly for LEECs, is that their emission can be readily tuned across the visible spectrum. In many cases, the emissive excited states of these complexes are a mixture of metal-to-ligand charge transfer (^{3}MLCT) between the metal and N^N ligands and ligand-to-ligand charge transfer (^{3}LLCT) between the phenyl rings of the C^N ligands and the N^N ligands. Thus, to a first approximation, the energies of the HOMOs and LUMOs of these complexes can be independently modulated as a function of appropriate substituent modification of the C^N and N^N ligands. Such facile colour tuning is in stark contrast to the narrow orange-red emission range of ruthenium(II) polypyridyl complexes. For reference, we include several reviews from other groups exploring colour tuning of iridium complexes.[5b, 8]

For LEECs, the major challenges that require addressing are the design of red and, especially, blue emitters. The emission colour perceived by the viewer is normally defined using the system of the Commission Internationale de l'Éclairage (CIE), which plots the

colour of the emission as a function of x and y coordinates. The CIE coordinates corresponding to deep blue are defined as (0.15, 0.06) while the saturated red coordinates are (0.60, 0.30). To date, no iridium-based emitter in a LEEC has come close to the required value for blue - the bluest reported CIE values are (0.20, 0.28)[9] - while there is only a single report of a deep blue emitting organic fluorophore used for LEECs (CIE: 0.15, 0.09).[10] For the red emitters, only four devices to date have been reported to display near the ideal red coordinate, but the lifetimes of these devices are very short ($t_{1/2}$ = 2.0 – 6.3 h, where $t_{1/2}$ is defined as the time taken for the luminance of the device to decay to half to the maximum).[11] Thus we have interests in tuning the emission of our complexes either to the red or to the blue.

Our main philosophy when undertaking any of our studies has been to start with understanding the basic properties of reference iridium complexes and then in a rational fashion design a suitable structure-property relationship study where we can establish trends in behaviour and so better understand these new systems. This is the manner in which we will approach this review, by exploring first the photophysics of archetypal iridium complexes **1** and **2** and then understanding how these properties change as the deviations in ligand structure from those present in these traditional complexes become increasingly elaborate. The strategies for tuning the photophysical properties of this class of iridium complexes will be illustrated largely using example studies coming out of our own group, as this will control for differences in measurement technique or instrumentation from one group to another, thereby producing a reliable comparison between different complexes.

We have often found density functional theory (DFT) calculations coupled with a strong background in physical organic chemistry to be useful tools in aiding us with our

interpretations and have used the insights gained to identify new emitters. However, even with the help of these tools, we have also on occasion found that the resultant photophysical properties we observe are in fact not what we might expect, which keeps this field of research both interesting and pertinent.

2: Archetypal Iridium Complexes.

In order to assess the effect of substitution/modification of the ligand scaffold about the iridium centre on the optoelectronic properties, it is necessary to define reference complexes from which to draw comparisons. The cationic iridium(III) complexes that best fit this purpose are the widely studied complexes **1** and **2**, whose photophysical properties were originally reported by Güdel *et al.*[12] We have collated all of the relevant photophysical properties of these two complexes in a recent review,[7b] and thus mention the salient features only briefly here.

Both complexes emit from a mixed ^{3}MLCT/^{3}LLCT state, luminescing yellow/orange light in MeCN (λ_{PL} = 602 nm for **1** and 588 nm for **2**; Φ_{PL} = 6 % for **1** and 23 % for **2**).[12e, 13] The modest blue-shift in the emission of **2** compared to **1** is due to the inductively electron-donating character of the *tert*-butyl groups, which destabilise the LUMO located on the ancillary N^N ligand as well as the first excited triplet state (T_1) of **2** compared to **1**. Structural deviation from these complexes is normally the result of one or more of three main substitutions: 1) modification of the aryl rings of the C^N ligands, 2) modification of the pyridyl or other heterocycle of the C^N ligands and 3) modification of one or both of the heterocycles of the N^N ligands (Figure **1**). We will study each of these three cases individually in the sections that follow, before investigating how combining substitution at multiple positions about the ligand scaffold can work in concert.

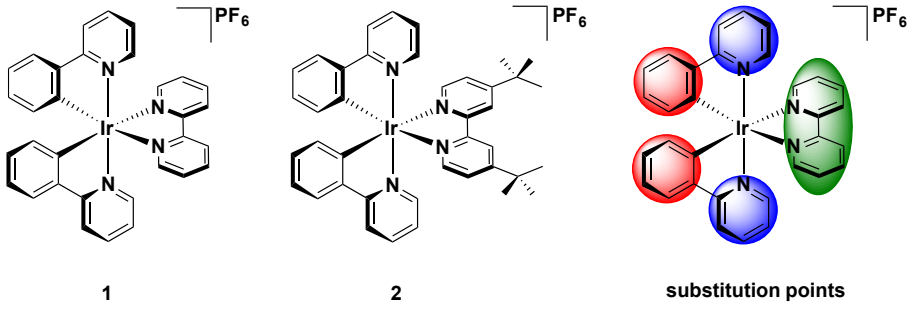

Figure **1**: Structures of $[Ir(ppy)_2(bpy)](PF_6)$, **1**, and its *tert*-butyl analogue, $[Ir(ppy)_2(dtbubpy)](PF_6)$, **2**, which are two of the most widely studied cationic iridium complexes. b) Distinct areas of **1** that are normally individually derivatised, where red is the phenyl ring of the C^N ligands, blue is the pyridyl rings of the C^N ligands and green is one or both of the pyridines on the N^N ligand. Substitution at each of these regions will be discussed individually, followed by combinations of substitutions.

Figure **2** illustrates the most common strategy for tuning the emission of heteroleptic cationic iridium complexes. The paradigm for emission tuning described in Figure **2** works for most, but not all complexes, of the form $[Ir(C^N)_2(N^N)]^+$. Density Functional Theory (DFT) calculations have shown that the HOMO is comprised of a mixture of the metal and the phenyl rings of the C^N ligands.[12d, 14] The LUMO is localised essentially exclusively on the bipyridine in both **1** and **2**. Thus, by adding the appropriate substituents to the ligands, the emission can conceivably be tuned from deep red to the blue. However, it is important to note that as the emission energy is tuned towards the extremities of the visible spectrum, the photoluminescence quantum yield, Φ_{PL}, of these complexes can often drop off precipitously. For example, the energy gap law states that the rate of non-radiative decay increases exponentially with decreasing emission energy as vibrational modes of the ground state more readily couple to those of the excited state,[15] which is the primary deactivation mode when tuning the emission towards the red. For iridium complexes that are being tuned towards

producing blue emission, the energies of the anti-bonding metal-centred (^{3}MC) and ^{3}CT (or ligand centred, ^{3}LC) are all very strongly destabilised. However, the relative destabilisation of the ^{3}MC states is less pronounced than the emissive ^{3}CT or ^{3}LC states, resulting in thermal population of these ^{3}MC states becoming increasingly likely as a function of an increasing HOMO-LUMO energy gap. Population of these ^{3}MC states leads to efficient and deleterious quenching of the emission.

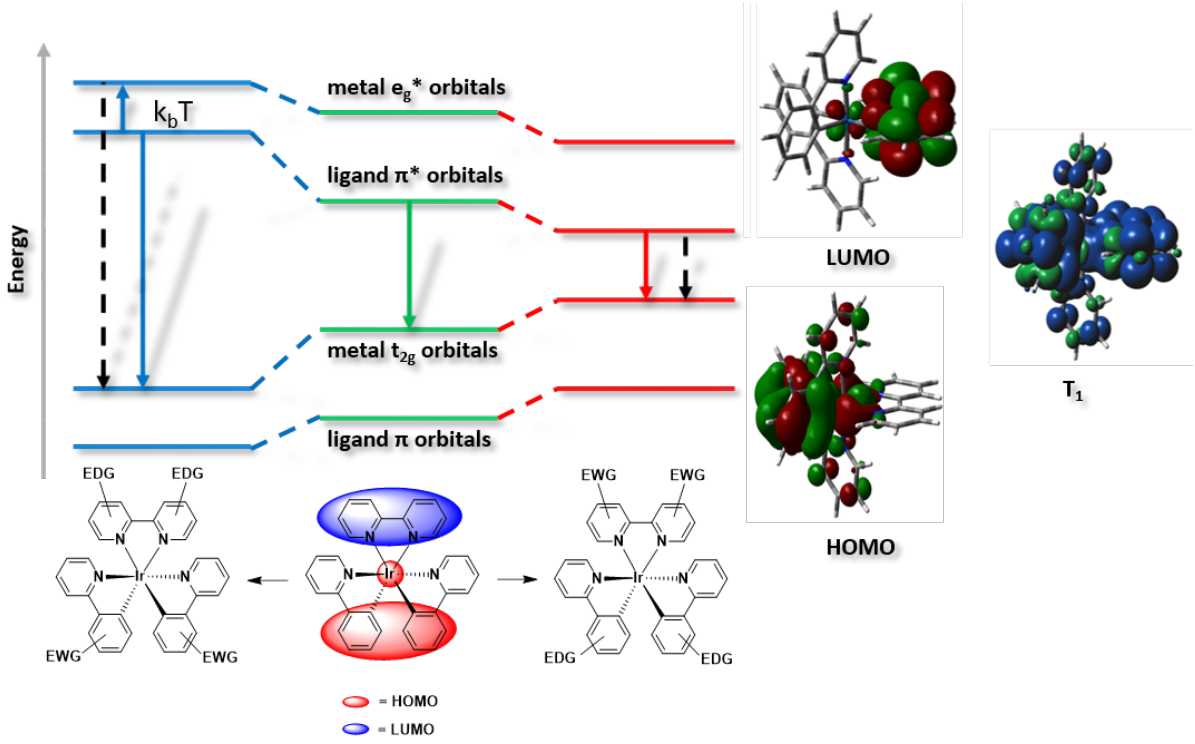

Figure **2**. General scheme depicting strategy for colour tuning the emission of $[Ir(ppy)_2(bpy)]^+$, **1**. DFT calculated Kohn-Sham MOs indicate an electron density distribution on the HOMO that is largely localised on the metal centre and the phenyl rings of the cyclometalating ligands, and on the LUMO that is largely localised on the bpy while the calculated spin density of the T_1 state is distributed across the entire molecule. This allows for tuning of the emission by appropriate functionalisation of the ligands. Dashed arrows indicate deactivation from the excited state via non-radiative decay. DFT [(B3LYP/SBKJC-VDZ for Ir(III)) and (6-31G* for C,H,N)] with CPCM (MeCN).

Aside from **1** and **2**, we will also consider two additional reference complexes in **3** and **4** that have significantly blue-shifted emission as a function of the fluorine atoms present on the C^N ligands, and thus are useful benchmarks for comparing new blue emitters. When designing complexes for blue emission, the most common strategy is to append electron-withdrawing substituents to the phenyl ring of the C^N ligands as this acts to lower the energy of the HOMO, thereby increasing the HOMO-LUMO gap and frequently leading to a blue-shift in the emission. Complex **3** employs the commonly used ligand 2-(2,4-difluorophenyl)pyridine (dFppy) wherein the presence of the two fluorine atoms act to strongly blue-shift the emission from the yellow-orange found in **1** and **2** to green (λ_{PL} = 515 nm for **3**; Φ_{PL} = 72 % in MeCN).[16] It is worth noting that in the LEEC device, this complex is among the most efficient emitters reported to date, with an external quantum efficiency (EQE) of 14.9 %.[17]

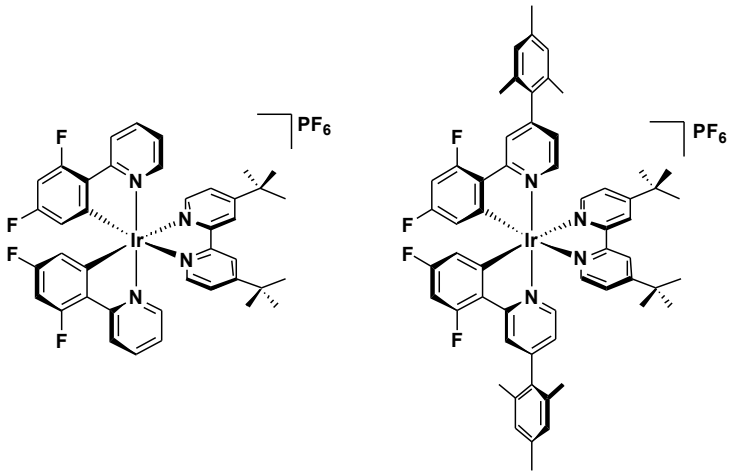

3 4

Figure **3**. Structure of [Ir(dFppy)$_2$(dtbubpy)](PF$_6$), **3**, which is a widely studied green-emitting iridium complex, and its mesityl-substituted analogue **4**, [Ir(dFMesppy)$_2$(dtbubpy)](PF$_6$), which shows the same electronic properties as **3** but with enhanced Φ_{PL}.

Complex **4** is the final reference complex, and it is structurally identical to **3** except for the addition of the mesityl units at the 4-position of the pyridine rings on the C^N ligands. This addition has no impact on the optoelectronic properties of the complex, as the mutually orthogonal conformation of the mesityl and pyridine rings disrupts any formal conjugation between the two. Furthermore, the steric bulk of the mesityl group inhibits intermolecular quenching of the emission in solution, resulting in an enhanced Φ_{PL} observed for **4** compared with **3**, while maintaining the same emission colour (λ_{PL} = 515 nm, Φ_{PL} = 80 % for **4**).[16] This mesityl substitution strategy was first reported by Bryce and co-workers[18] and we have since found it to be applicable to a wide variety of systems, many of which will be discussed here.

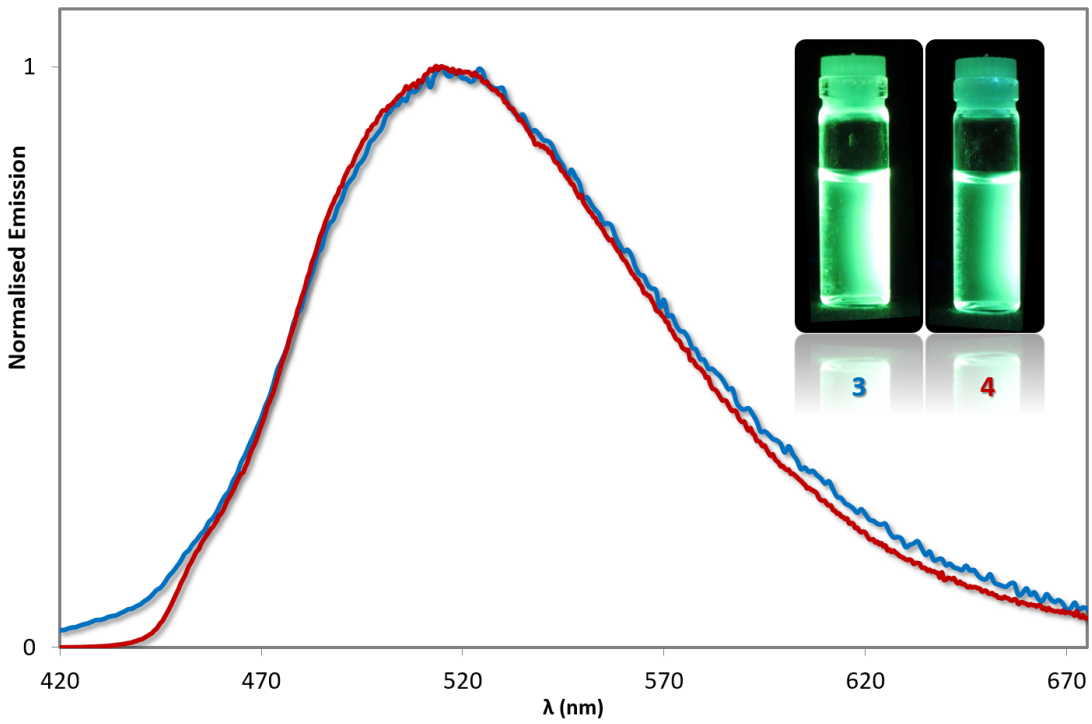

Figure **4**. Emission spectrum of **3** and **4** in MeCN solution. Inset: photograph of MeCN solutions of **3** and **4** showing their green colour under UV photoexcitation.

3: C^N Ligand – Effects of Substitution on the Phenyl Ring.

In this section we will explore the effect on the photophysics of the complex when the C^N ligand is substituted with electron-withdrawing or electron-donating functionalities. Of

particular importance here is the regiochemistry of the substituent with respect to the Ir-C bond. Hammett values ($\sigma_{m/p}$), which parameterise the electron-withdrawing or donating character of a substituent based on whether it is situated in a *meta* or *para* position to a particular functional group of interest, are useful tools in understanding these electronic effects, although there are instances where these relationships break down.[19] We note that Baranoff and co-workers have established a quantifiable relationship between Hammett values and several optoelectronic properties of neutral iridium(III) complexes.[20]

Many groups have explored incorporating electron-withdrawing substituents onto the C^N ligands in place of or in addition to fluorine atoms with the goal of blue-shifting the emission.[21] Several examples of these groups include: trifluoromethyl,[22] sulfonyl,[23] phosphonium,[24] diarylphosphine oxide[23b] and nitrile.[21, 25] In addition, there have also been efforts to change the aryl ring of the C^N ligands altogether from phenyl to a heterocycle such as pyridine,[26] pyridinium[27] or even pyrimidine.[28] The nitrogen atoms in these heterocycles stabilise the HOMO by inductively withdrawing electron density away from the metal centre (Figure **5**).

Although many blue-emitting iridium complexes that are reported contain fluorine atoms appended to the C^N ligands, there has been a concerted effort to move away from fluorinated C^N ligands. The F-C_{aryl} bond has been identified as a point of electrochemical instability in these complexes, especially when placed on the C^N ligands, as this can activate the ring to degradation by such processes as nucleophilic aromatic substitution in the device.[29] Exploring new and more chemically robust functional groups or heterocylic rings is thus an important avenue of research. Complexes **5**, **6**, **7** and **11** are some examples of blue to

sky-blue-emitting complexes reported that do not contain F-C_{aryl} bonds while complexes **8-10** combine both fluorine and other electron-withdrawing groups on the C^N ligands.

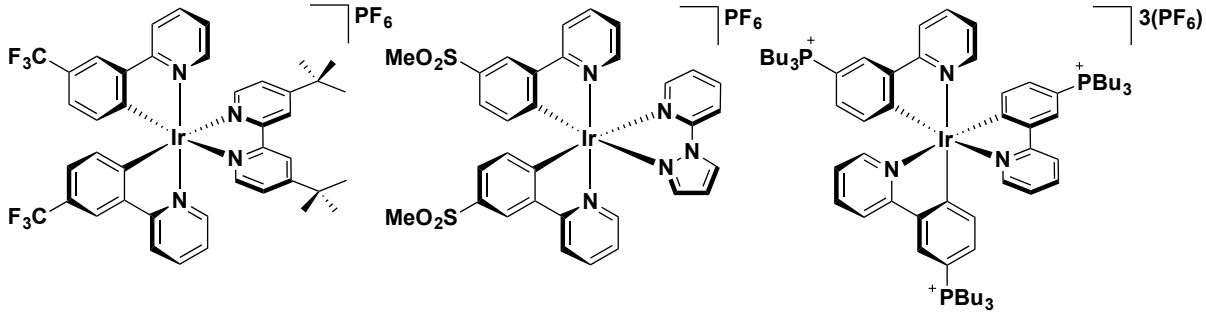

5
J. Mater. Chem. C, 2013, **1**, 2241.
λ_{PL}: 512 nm
Φ_{PL}: 66%

6
RSC Adv., 2015, **5**, 42815
463, 493 nm
72%

7
Chem. Mater., 2006, **18**, 2778
480 nm
34%

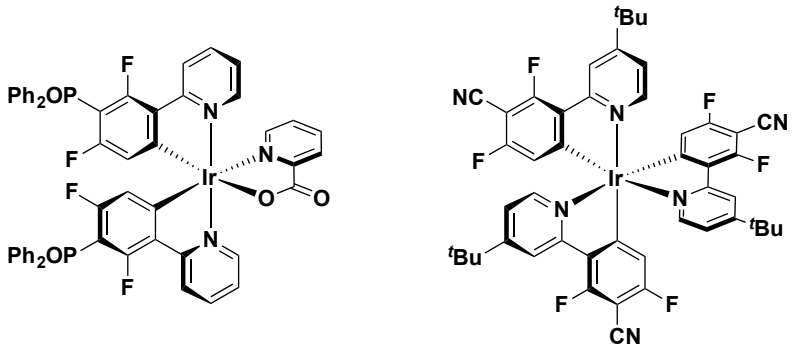

8
Chem. Mater., 2012, **24**, 4581.
λ_{PL}: 460, 489 nm
Φ_{PL}: 49%

9
Adv. Opt. Mater., 2015, **3**, 211
451, 476 nm
61%

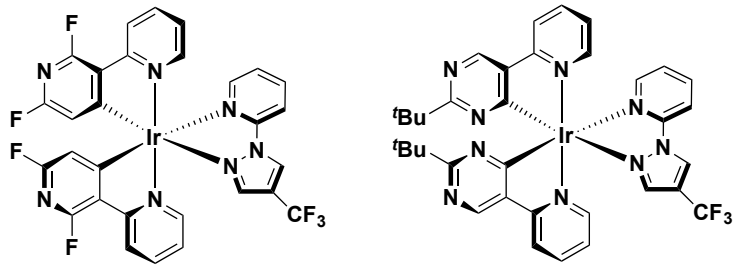

10
Chem. Mater., 2012, **24**, 3684.
λ_{PL}: 440, 469 nm
Φ_{PL}: 79%

11
ACS Appl. Mater. Interfaces, 2013, **5**, 7341
456, 488, 521 nm
62%

Figure **5**. Literature examples of different blue-to-sky-blue-emitting iridium complexes for use in LEECs (**5** – **7**) or OLEDs (**8** – **11**). Their relevant photophysical properties in DCM (**5**, **8**, **11**) MeCN (**6**, **7**), chloroform (**9**) or 2-MeTHF (**10**) solution are given for reference.

We have also targeted strongly electron-withdrawing substituents with large Hammett values as a strategy to blue-shift emission. Complexes **12** – **15** are four examples that contain trifluoromethyl-type substituents at the 4-position of the cyclometalating phenyl ring. Our recent study explored whether spacing the trifluoromethyl unit with oxygen (**13**), sulfur (**14**) or sulfonyl (**15**) would lead to an increased blue-shift in the emission compared to that observed for the reference complex **12**. The emission maxima of the complexes correlated only somewhat to their corresponding Hammett values of the four functional groups, despite their HOMO energies being strongly correlated. We observed that for complexes **12** – **14**, the emission maxima (λ_{PL} = 484, 516 nm for **12**, 527 nm for **13** and 491, 525 nm for **14**, in MeCN) followed the trend of the Hammett values (σ_m = 0.43, 0.38 and 0.40 for **12**, **13** and **14**, respectively), with **12** the bluest of these complexes. However, to our surprise, complex **15**, which has the most electron-withdrawing substituent (σ_m = 0.83 for the -SO_2CF_3 group), is in fact the most *red-shifted* of the four complexes (λ_{PL} = 515, 545 nm), illustrating the limits of this approach.

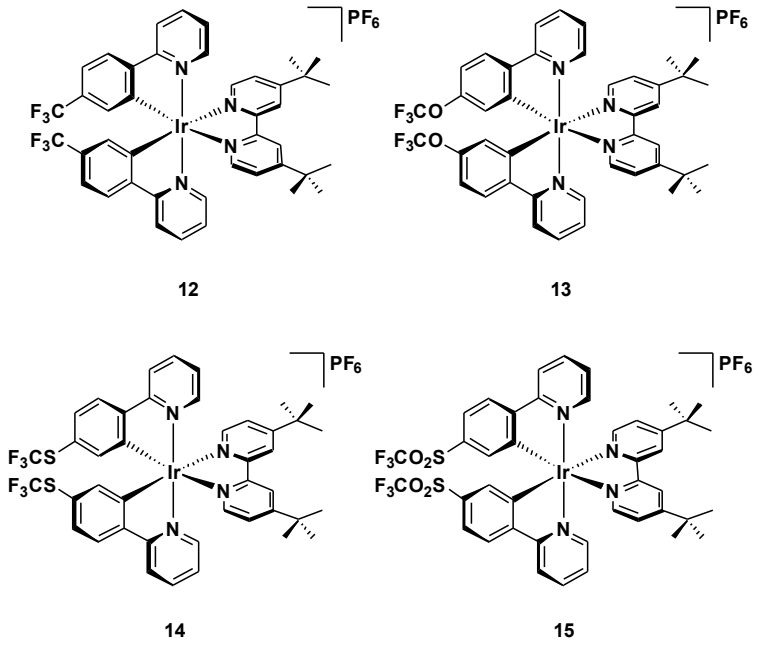

Figure **6**. Iridium complexes bearing a variety of trifluoromethyl-type substituents on the C^N ligands.

Another strongly electron-withdrawing substituent that we have studied is the pentafluorosulfanyl group (–SF_5), which possesses a large associated Hammett value (σ_m = 0.61, σ_p = 0.68). These substituents are underexplored as motifs in coordination compounds despite their extensive use in medicinal and materials chemistry applications.[30] Complexes **16** – **19** represent the first examples of iridium complexes bearing –SF_5 substituents.[31]

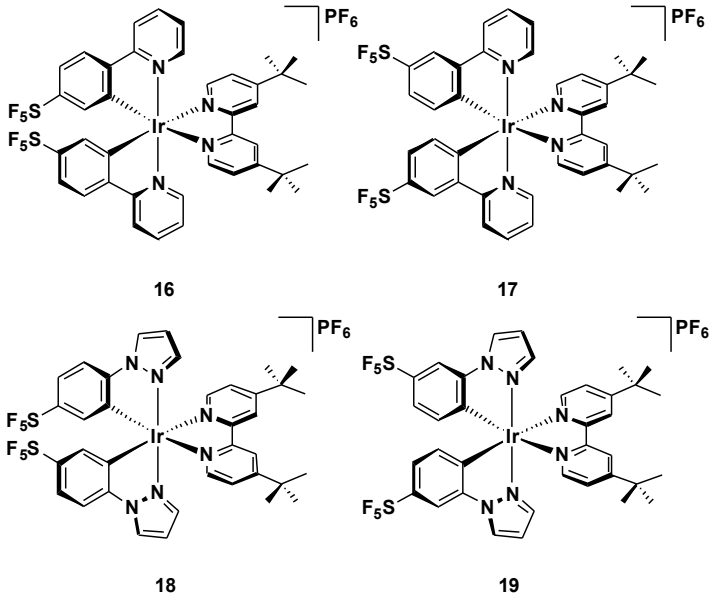

Figure **7**. Iridium complexes bearing pentafluorosulfanyl substituents on the C^N ligands.

All four complexes emit blue-green light that is modestly blue-shifted compared to **3** in MeCN solution (λ_{PL} = 485 – 503 nm). We were surprised to find that of these four complexes, **16** shows the bluest emission profile. This observation goes against two generally accepted substitution paradigms employed for blue-shifting the emission of these materials. Firstly, substituting pyridines for more electron-rich heterocycles, such as pyrazoles, on the C^N ligands generally blue-shifts emission due to the increased π-accepting character of this ring, which leads to a stabilisation of the HOMO.[11d] Indeed, we observed by cyclic

voltammetry that this predicted electronic tuning was operational, with the pyridyl complexes showing lower positive oxidation potentials (E_{ox} = 1.57 V for **16** and 1.58 V for **17**, *vs* SCE) than their pyrazole analogues (E_{ox} = 1.64 V for **18** and 1.67 V for **19**, *vs* SCE). These observations point to the difficulty of correlating electrochemistry – a ground state experiment – with the excited state properties characterised by emission.[32] Secondly, we also unexpectedly observed that the *meta* regiochemistry of the $-SF_5$ unit to the Ir-C bond in **16** actually produced a greater blue-shift than the *para* relationship in **17** when frequently the opposite trend is observed (*c.f.* Hammett values for a measure of the relative electron-withdrawing power of the group).[23a, 27a]

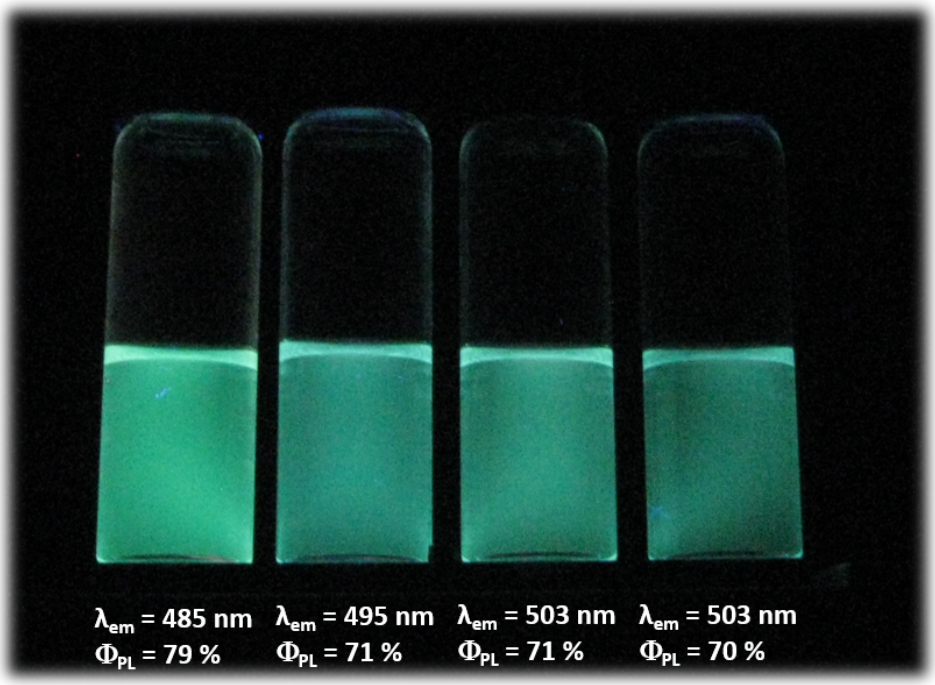

Figure **8**. Emission in solution of complexes **16** – **19** (in order from left to right) in MeCN.

Although these complexes showed reasonably reversible oxidation waves (attributable to the Ir^{III}/Ir^{IV} redox couple), the reductions of all four complexes, in the region of -1.30 to -1.40 V *vs* SCE, are multi-electron and highly irreversible in nature, which was attributed to direct electrochemical decomposition of the $-SF_5$ unit. This is compared with that of **3** (E_{red} = -1.36

V *vs* SCE), which shows good reversibility characteristic of reduction of the bpy ligand to its radical anion.[16] The absence of electroluminescence in the LEEC devices was attributed to the electrochemical instability of these complexes, since the emitters in LEECs are required to perform the dual role of light emission and charge transport, the latter of which requires electrochemical reversibility to be effective. By contrast, these compounds exhibited green electroluminescence in solution-processed OLEDs (EQE = 0.2 – 1.7%), since the role of charge transport is instead handled primarily by the molecules of the host matrix within the emissive layer.

Similarly to complexes **10**,[26d] **11**[28a] and others,[26a-c, 28b] we have also explored replacing the phenyl ring for a cyclometalating heterocycle (complexes **20** – **23**). The presence of the nitrogen atom *para* to the Ir-C bond leads to a strong stabilisation of the HOMO energy and is primarily responsible for the blue-shifted emission in solution (λ_{PL} = 510 – 517 nm in MeCN for **20** – **23**).[33] Although not observed in solution for this family of complexes, others have shown that alkoxy groups are useful substituents in blue-shifting the emission.[20, 26c, 28b] While their *para* Hammett values are negative (σ_p = -0.27), in a *meta* position these values are positive (σ_m = 0.61), allowing for stabilisation of the HOMO through inductive electron-withdrawing effects.

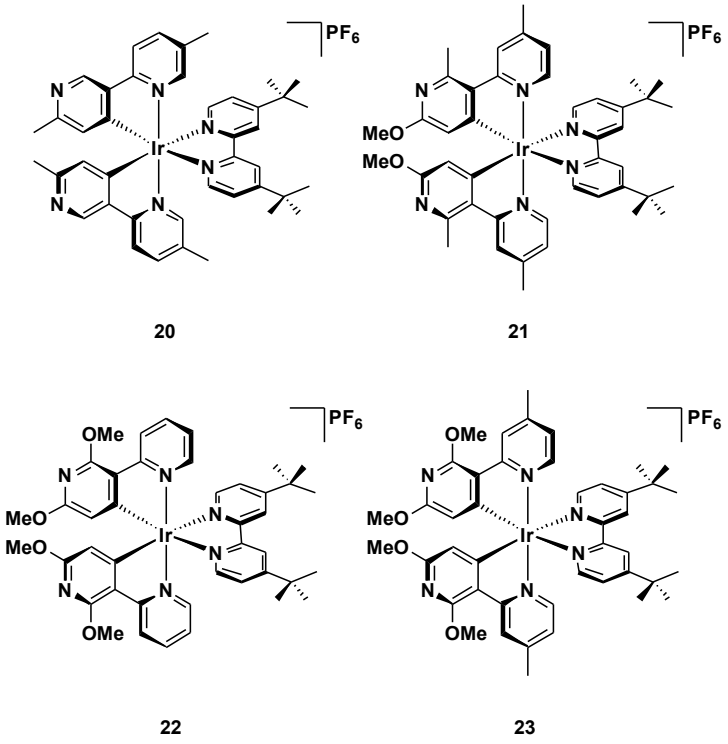

Figure **9**. Iridium complexes based on cyclometalated 2,3'-bipyridines.

In the neat film the emission of **20** is strongly red-shifted (λ_{PL} = 547 nm) compared to **21** – **23** (λ_{PL} = 514 – 525 nm) and is also significantly less emissive (Φ_{PL} = 2%) compared with the other three complexes (Φ_{PL} = 19–32%) suggesting that in addition to maintaining bluer emission, the added steric bulk of the methoxy groups helps to reduce concentration quenching in the neat film. It is worth noting that there is still a lack of understanding regarding the changes in the photophysical properties when transitioning from solution to solid state, and this is a topic that requires addressing in future molecular design of emitters for LEEC devices, where packing in the film becomes important. Ultimately, this leads to poor LEEC device performance for **20**, but better LEEC efficiencies for complexes **21** – **23** (EQE = 2.0 – 2.8%), as well as emission very close to the ideal green CIE coordinate (CIE: 0.30, 0.60) for complex **21** (CIE: 0.31, 0.57).

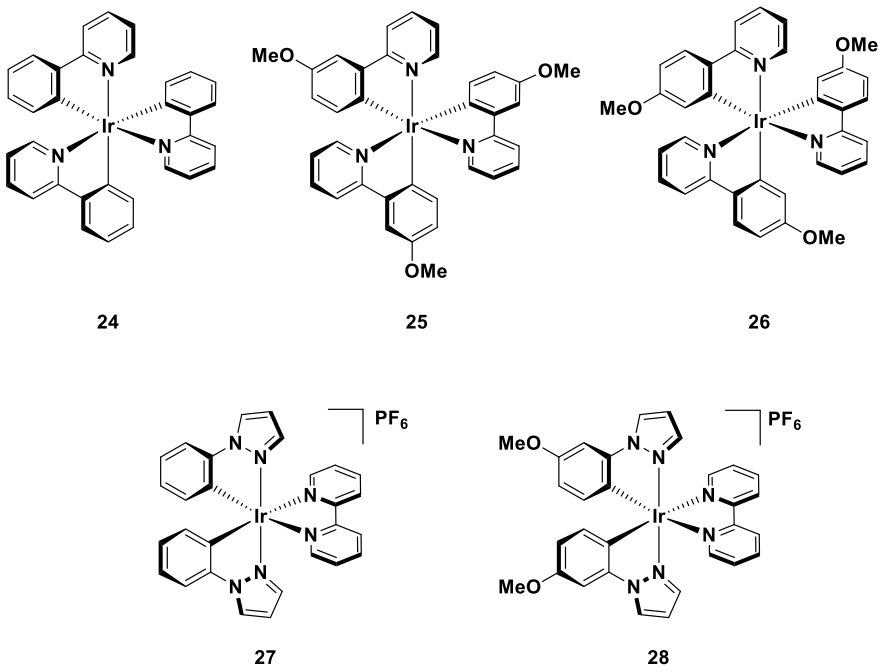

24 25 26

27 28

Figure **10**. Neutral (**24**) and charged (**27**) reference complexes to MeO-substituted neutral (**25** and **26**) and charged (**28**) iridium complexes.

Despite the many examples reporting the use of alkoxy groups for blue-shifting emission, the 'intuitive' strategy of using these groups to red-shift emission has in fact not been widely explored. An early example of the use of methoxy groups to mesomerically red-shift emission was reported by Watts *et al.*,[34] who showed that the emission of the tris-cyclometalated complex *fac*-[Ir(ppy)$_3$] (**24**) could be red-shifted if -OMe groups were appended *para* to the Ir-C bond (**25**) or blue-shifted if they were in a *meta* relationship (**26**) to the iridium centre (λ_{PL} = 494 nm for **24**, 539 nm for **25** and 489 nm for **26** MeOH/EtOH glass at 77 K). More recently, Davies and co-workers[35] reported a family of iridium complexes bearing 1-phenyl-1*H*-pyrazole (ppz) and various ppz derivatives as C^N ligands. They observed that compared to the reference complex **27** (**27**, λ_{PL} = 557 nm in DCM) the complex bearing -OMe groups, **28**, displayed a strongly red-shifted emission (**28**, λ_{PL} = 615 nm in DCM).

Our study explored decoration of the C^N ligands with an increasing number of –OMe groups in a systematic fashion to red-shift the emission and explore the competing σ-withdrawing effects with the π-donating effects of these substituents (**29a** – **32b**).[36] The emission profiles of **29a** and **29b** are the most blue-shifted in the study (λ_{PL} = 618 and 595 nm for **29a** and **29b** in MeCN, respectively) but nevertheless are red-shifted compared with **1** and **2** (λ_{PL} = 602 and 585 nm for **1** and **2** in MeCN, respectively). For complexes **30a** and **30b**, the importance of the substitution regiochemistry becomes clear, with the emission of these compounds greatly red-shifted (λ_{PL} = 710 and 680 nm for **30a** and **30b** in MeCN, respectively) compared to **29a** and **29b**. For these two complexes, the mesomeric effects of the –OMe groups govern the emission energy. The situation with complexes **31a** – **32b** is somewhat less clear. Complexes **31a** and **31b** are the most red-shifted among all eight of this family (λ_{PL} = 730 nm for **31a** and 700 nm for **31b**), but this red-shift is only relatively small compared to the large red-shift in emission achieved by the substitution at the 5-position of the phenyl rings in **30a** and **30b**. Furthermore, adding a third -OMe substituent induces a small blue-shift (λ_{PL} = 720 nm for **32a** and 685 nm for **32b**), in a somewhat analogous fashion to the photophysical properties of the emitters **20** – **23**.

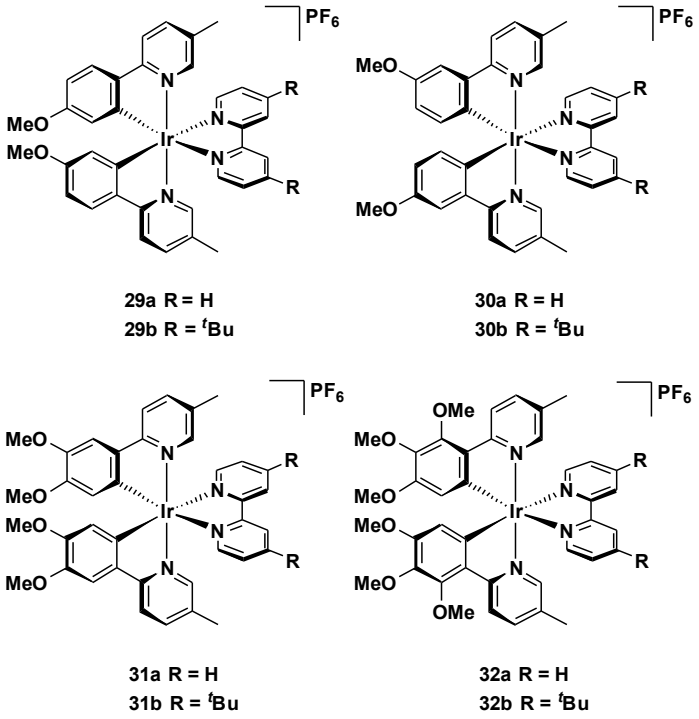

Figure **11**. Cationic iridium complexes bearing an increasing number of methoxy substituents on the C^N ligands.

The electrochemistry follows the trend found for the emission properties. For all of these complexes, the reduction is largely unchanged compared to **1** and **2**, pointing towards emission tuning being a HOMO-dominated effect. Accordingly, there is stark contrast in the oxidation potentials, which vary significantly across the series. The most stabilised values were observed for **29a** and **29b** (E_{ox} = 1.15 and 1.13 V *vs* SCE, for **29a** and **29b**, respectively), whereas the most red-shifted emitters, **31a** and **31b** also showed the lowest oxidation potentials (E_{ox} = 0.84 and 0.78 V *vs* SCE, for **31a** and **31b**, respectively). Apart from **29a** and **29b** (Φ_{PL} = 6 and 15% for **29a** and **29b** in MeCN, respectively), all of these complexes were poorly emissive (Φ_{PL} < 1%) presumably as a result of the energy gap law. Thus, in the LEECs their performances were limited, with **31b** showing the best device performance (EQE = 0.05 %, $t_{1/2}$ = 2 h, CIE: 0.61, 0.38). These numbers are low compared to

champion orange-red LEECs in terms of efficiencies (EQE = 3.3 – 9.5%)[11b, 11d, 37] and device lifetimes ($t_{1/2}$ = 10 – 37 h)[37-38] reported for this colour.

To conclude this section, the features to note concern the crucial role that regiochemistry of the substituents on the C^N ligands plays in influencing the photophysics of these complexes, and how this can (in a large number of cases) be correlated with the corresponding Hammett values of the substituent. Furthermore, when there are multiple substituents on the C^N ligands the emission can be tuned further, but the effects on the photophysics are not necessarily linearly additive with each substituent added, making their influence sometimes difficult to discern.

4: C^N Ligand – Effects of Substitution/Modification of the Pyridyl Ring

Rather than decorating the pyridyl ring of the C^N ligands with substituents, modification of this ring is typically achieved by utilising an entirely different heterocycle. To the best of our knowledge, the most common ligand framework used to this end is 1-phenyl-1*H*-pyrazole (ppz). By electrochemistry, it has been demonstrated that the second nitrogen atom in the five-membered heterocycle blue-shifts emission through stabilisation of the HOMO of these complexes.[11d, 23a, 23c, 39] Other C^N ligands coordinated to iridium(III) containing nitrogen-rich heterocycles such as imidazoles;[40] 1,2,3-triazoles;[41] 1,2,4-triazoles;[42] and 1,2,3,4-tetrazoles[43] have also been reported, and an important feature to note from these studies is that they do not always modulate the HOMO energy. In particular we will show that 1,2,3-triazoles strongly influence the LUMO energy instead. For reference, we point the reader to Ortí and co-workers' recent extensive theoretical study into the effect on the photophysical properties of varying the nitrogen count and regiochemistry of a wide variety of different C^N ligands.[44]

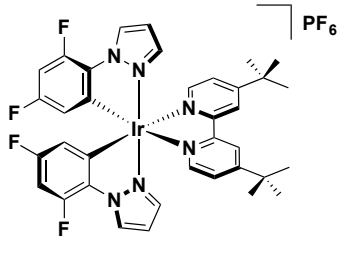

32

Org. Electron., 2012, **13**, 483.

λ_{PL}: 492 nm

Φ_{PL}: 100 %

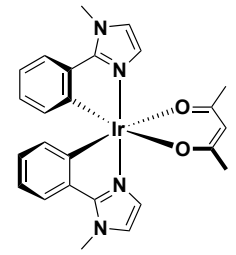

33

Chem. Commun., 2009, 4672

570 nm

2 %

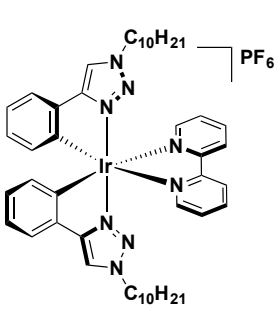

34

Organometallics, 2009, **28**, 5478.

λ_{PL}: 560 nm

Φ_{PL}: 45 %

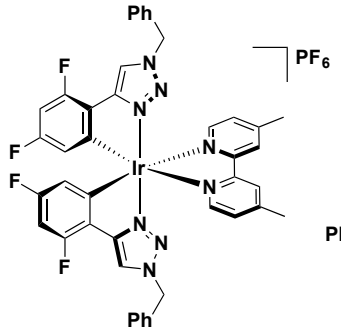

35

J. Am. Chem. Soc., 2011, **133**, 10543

497 nm

81 %

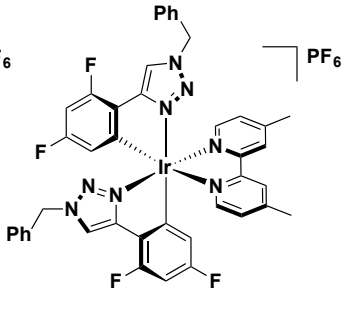

36

512 nm

77 %

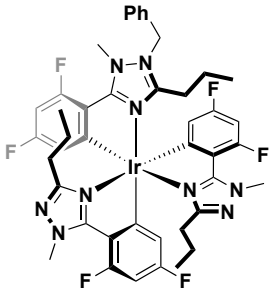

37

Chem. Mater., 2006, **18**, 5119.

λ_{PL}: 425, 450 nm

Φ_{PL}: 3 %

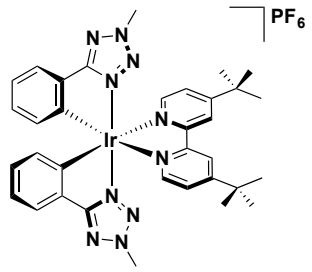

38

Inorg. Chem., 2014, **53**, 7709

530 nm

68 %

Figure **12**. Iridium complexes bearing a variety of different azoles within the C^N ligand framework. Their relevant photophysical properties in DCM (**33 – 35**) MeCN (**36**, **37**, **39**) and toluene (**38**) solution are given for reference.

We have shown theoretically that phenyl-1,2,3-triazole (phtl) ligands, such as those used in complexes **35** – **37**, are important nitrogen-rich C^N ligands that can blue-shift emission..[45] We studied the complexes in Figure **13**, using 1-benzyl-4-phenyl-1*H*-1,2,3-triazole (phtl,

complexes **40a** and **40b**) and 1-benzyl-4-(2,4-difluorophenyl)-1*H*-1,2,3-triazole (dFphtl, complexes **41a** and **41b**).

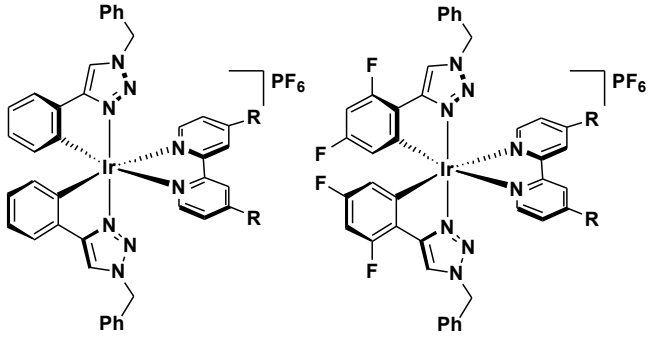

Figure **13**. Iridium complexes bearing 1,2,3-triazoles within the cyclometalating C^N ligand framework.

In contrast to ppz, which stabilises the HOMO, we observed that these phtl ligands intrinsically tune the LUMO, despite the LUMO showing electron density largely localised on the ancillary N^N ligand. Consider the electrochemical data shown in Table **1**. Comparing the HOMO energies of **2** with **40b** (E_{HOMO} = -5.71 eV for **2** and -5.66 eV for **40b**) or **3** with **41b** (E_{HOMO} = -6.02 eV for **3** and -6.00 eV for **41b**) shows that the HOMO is rather insensitive to modification of the coordinating heterocycle of the C^N ligands. By contrast, the LUMO changes significantly, with the LUMOs of **40b** (E_{LUMO} = -2.88 eV) and **41b** (E_{LUMO} = -2.95 eV) strongly destabilised compared with their pyridyl analogues (E_{LUMO} = -3.04 and -3.06 eV for **2** and **3**, respectively). Although the effect on the HOMO energies is non-zero, demonstrating that with all these substitutions one is never exclusively modulating the energy of only one set of orbitals without affecting the other set, this design strategy clearly produces a LUMO dominant effect. DFT computations reveal a non-zero orbital contribution from the

metal to the LUMO, which accounts for the strong sensitivity of the LUMO to the nature of the heterocycle on the C^N ligand.

Table **1**.[a,b] Electrochemical data comparing complexes bearing pyridyl (**2** and **3**) and 1,2,3-triazoles (**40b** and **41b**) within the C^N ligand framework.

		$E_{1/2}$ (V vs SCE)		$E_{orbital}$ (eV)		Ref
Complex	C^N Ligand	E_{ox}	E_{red}	HOMO	LUMO	
2	ppy	1.29	-1.38	-5.71	-3.04	[13a]
3	dFppy	1.60	-1.36	-6.02	-3.06	[16]
40b	phtl	1.24	-1.54	-5.66	-2.88	[45]
41b	dFphtl	1.58	-1.47	-6.00	-2.95	[45]

[a] Measurements were carried out in de-aerated MeCN and are referenced *vs* SCE (Fc/Fc^+ = 0.38 in MeCN).[46] [b] $E_{HOMO/LUMO} = -[E^{ox/red}_{vs\ Fc/Fc+} + 4.8]$ eV.[47]

The photophysical data also demonstrate the blue-shifting nature of the triazoles. The emission maxima of **40a** and **40b** (λ_{PL} = 580 and 575 nm, respectively in MeCN) are blue-shifted compared to **1** and **2** (λ_{PL} = 602 and 591 nm, respectively in MeCN). The addition of fluorine atoms to the C^N ligands blue-shifts the emission further, with **41b** showing sky-blue emission, rather than the green emission of **3** (see Figure **14**; λ_{PL} = 515 nm for **3** and 498 nm for **41b**).

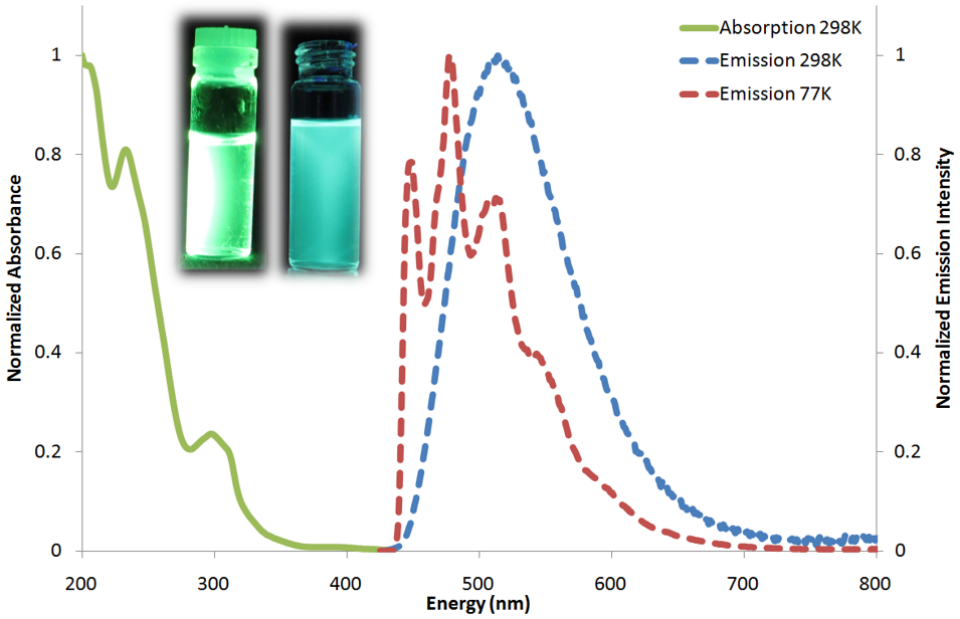

Figure **14**. Relevant photophysical data for **41b** in MeCN. Inset: emission in solution of **3** (left) and **41b** (right) to demonstrate blue-shift achieved by substituting the pyridyl ring on the C^N ligand for a 1,2,3-triazole ring.

An important consideration then is *how* employing a different heterocycle to pyridine in the C^N ligands tunes the emission. We have striven to show here that this is not immediately obvious, with pyrazoles exerting HOMO-tuning effects and triazoles modulating the LUMO. These are important considerations that should inform future molecular design.

5: N^N Ligand – Effect of Substitution/Modification of the bpy

In this section, we explore different ways of modifying the N^N ligand to shift the emission either to the blue or to the red. These strategies are based on the fact that the LUMO is typically localised on this ligand. For shifting the emission towards the blue, there are two main strategies designed to raise the energy of the LUMO. The first strategy, which will be discussed in Section 6, is to decorate bipyridines with strongly electron-donating groups such as amines. The second, and demonstrably more fruitful strategy, involves replacing the

coordinating pyridine rings with more strongly σ-electron donating heterocycles, as has been reported with the complexes **42** – **46**. This second strategy will be the main focus of this section. Red emission, by contrast, can be accomplished in one of two main ways: 1) appending electron-withdrawing groups onto the N^N ligand to stabilise the LUMO; or 2) increasing the conjugation of the N^N ligands to narrow the HOMO-LUMO gap, Examples of both strategies will be highlighted here.

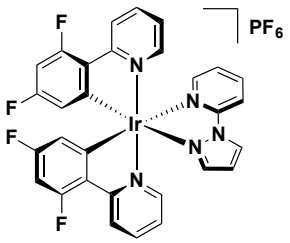

41
Adv. Funct. Mater., 2008, **18**, 2123.
λ_{PL}: 451, 484 nm
Φ_{PL}: 20 %

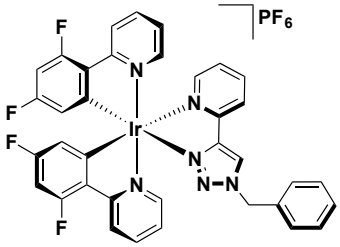

42
Adv. Funct. Mater., 2010, **20**, 1812.
452, 483 nm
22 %

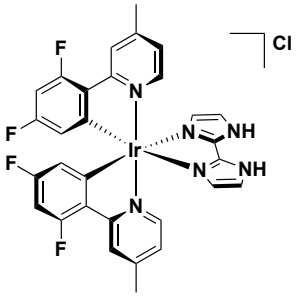

43
Bull. Korean Chem. Soc., 2012, **33**, 3645.
λ_{PL}: 456, 484 nm
Φ_{PL}: 10 %

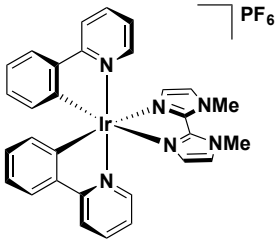

44
Adv. Funct. Mater., 2009, **19**, 2950
496 nm
5 %

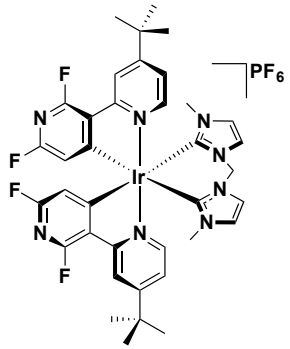

45
J. Mater. Chem. C, 2013, **1**, 58.
λ_{PL}: 440 nm
Φ_{PL}: 13 %

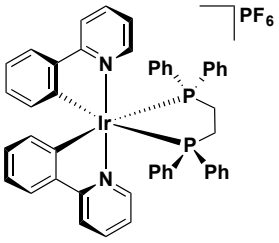

46
Polyhedron., 2012, **35**, 154
459 nm
0.4 %

Figure **15**. Blue-emitting iridium complexes with modified ancillary ligands. Photophysics reported in MeCN (**42**, **45** – **47**) or DCM (**43**, **44**).

Given the efficacy of triazoles in blue-shifting emission for complexes **40a** – **41b**, we wanted to explore their effects when incorporated within the ancillary ligand. De Cola and co-workers[48] showed that using these heterocycles as part of the ancillary ligand framework is even more effective in blue-shifting the emission than when they are incorporated within the C^N ligands. This enhanced tuning effect is not specific to 1,2,3-triazoles and has also been shown for other heterocycles as well. Indeed, comparing, for example, otherwise analogous complexes wherein pyrazole rings have been included into the ligand framework either of the N^N ligand (**42**) or the C^N ligands (**33**), the complex bearing the modified N^N ligand generates an invariably bluer emission (λ_{PL} = 452, 480 nm for **42** and 492 nm for **33**).[7b, 9, 39c] Thus we designed complex **48**, which employs a bis(triazole), btl, ancillary ligand. As with **43**, inclusion of triazole motifs on the N^N ligand, rather than the C^N ligands produced an even more pronounced destabilization of the LUMO.[49] Complex **48** shows structured LC-type emission (λ_{PL} = 481, 511 nm) while the emission spectra of **40a** and **40b** are broad, unstructured and substantially red-shifted in colour (λ_{PL} = 580 and 575 nm, respectively) and predominantly CT in nature. Achieving such a large blue-shift in the emission without concomitant modification of the C^N ligands is normally difficult, and important when pursuing fluorine-free blue emitters. Attempts to further blue-shift the emission through judicious decoration of the C^N ligands however produced photochemically unstable complexes (see section **7**).

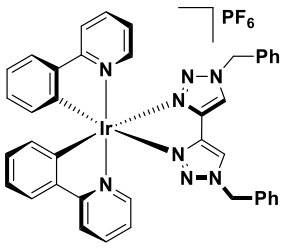

48

Figure **16**. Iridium complex bearing a bis-1,2,3-triazole ancillary ligand.

In a similar fashion to the btl ligand, biimidazole (biim) ligands are also effective scaffolds for blue-shifting emission of cationic iridium complexes. The potency of both the parent 1*H*,1*H*'-2,2'-biimidazole (H_2biim)[50] and the dimethylated analog 1,1'-dimethyl-2,2'-biimidazole (Me_2biim)[11a] had previously been demonstrated with complexes **44** and **45** emitting in the blue-green to blue regime in MeCN solution, respectively. However, both **44** (Φ_{PL} = 10% in DCM) and **45** (Φ_{PL} = 5% in MeCN) were poorly emissive. In addition, the high orbital energies associated with these biimidazole-type N^N ligands renders them essentially 'non-chromophoric' in nature, resulting in both complexes displaying predominantly LC-type emission localised on the C^N ligands rather than mixed MLCT/LLCT emission that typically characterises complexes such as found for **3**. This interplay between MLCT/LLCT and LC excited states is a common feature of blue-emitting complexes with modified ancillary ligands.

We hypothesized that the reason for the low Φ_{PL} was due to the presence of an undesired twisting of the biimidazole in the excited triplet state, which would subsequently twist back into planarity upon relaxation to the ground state *via* a non-radiative pathway.[51] DFT modelling supported this proposal whereby in particular the steric bulk of the methyl groups in **50** enforced a twisting out of planarity of the ancillary ligand (Figure **16**). Indeed, both **49**

and **50** show blue, ligand-centred emission (λ_{PL} = 464, 490 nm for **49** and 457, 486 nm for **50**, in MeOH) but with expectedly low photoluminescence quantum yields (Φ_{PL} = 20% for **49** and 2% for **50**) and short emission lifetimes (τ_e = 1.6 μs for **49** and just 91 ns for **50**), particularly considering the LC nature of the emission. In order to mitigate this non-radiative pathway, we proposed that a strategy to tether the distal nitrogen atoms of the ancillary ligands could rigidify the ligand framework and thus restrict the distortions observed for **50** in the excited state. Our lead candidate was **51**, which, aside from the rigidity imparted by the *o*-xylylene linker, was also predicted to maintain the same optoelectronic properties, since the methylene groups impede further conjugation between the tethered phenyl group and the remainder of the ligand framework.

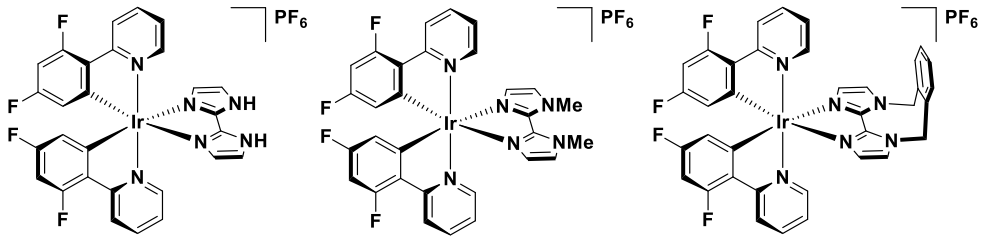

Figure **17**. Iridium complexes bearing various biimidazole-type ligands.

The emission of **51** in MeOH showed essentially the same profile and energy as that of **50**. More importantly, and gratifyingly, the Φ_{PL} of **51** was greatly enhanced (Φ_{PL} = 68%) compared to both **49** and **50**, demonstrating the viability of this strategy and corroborating our hypothesis. The emission lifetime of **51** (τ_e = 3.8 μs) was also significantly longer than that observed for either **49** or **50**. By comparison, the τ_e at 77 K for all three complexes are all similar (τ_e = 3.7 – 4.0 μs for **49** – **51**) suggesting that the rigidified local environment at low temperature impedes any distortions of the biimidazole from occurring and thus further

substantiating our assertions that quenching of **49** and **50** is attributable to vibrational processes.

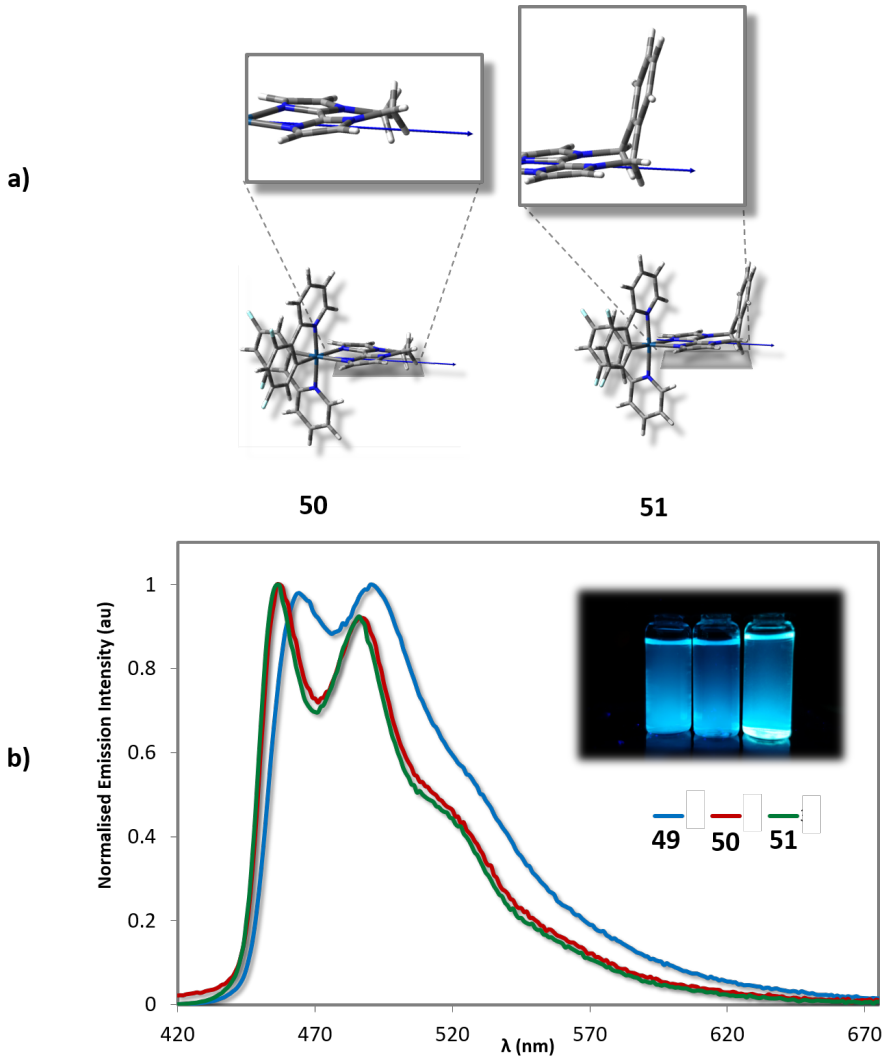

Figure **18**. a) Calculated geometries of **50** and **51** in the T_1 state, with zoomed images showing the distortion of the biimidazole invoked by the steric bulk of the clashing methyl groups (**50**) and the lack of such distortion when tethered (**51**). DFT [(B3LYP/SBKJC-VDZ for Ir(III)) and (6-31G* for C,H,N)] with CPCM (MeCN). b) Emission spectra of **49** – **51** in deaerated MeOH, with the emission colour in solution inset.

Although this strategy proved effective, the poor solubility of **51** in most organic solvents precluded its viability as a solution-processable emitter for LEECs. We thus targeted a

mesitylated analogue based on a design similar to **4** (Figure **19**).[16] Complex **52** is both more soluble in polar organic solvents, and also more emissive in solution (Φ_{PL} = 82% in MeOH and 90% in MeCN) than **51**. This Φ_{PL} value for a cationic blue emitter (λ_{PL} = 459 nm) in solution is among the highest ever reported.[9, 11a, 52] The architecture of **52** demonstrates the importance of rational ligand design that combines elements to effectively tune the electronics of the complex with control over *intramolecular* quenching processes (the tethered biimidazole) and *intermolecular* quenching processes (the bulky mesityl substituent). This complex was studied in solution-processed OLEDs, giving sky blue emission (CIE: 0.21, 0.37) and reasonable efficiency (EQE = 3.42%) for a cationic complex employed in an OLED.[16]

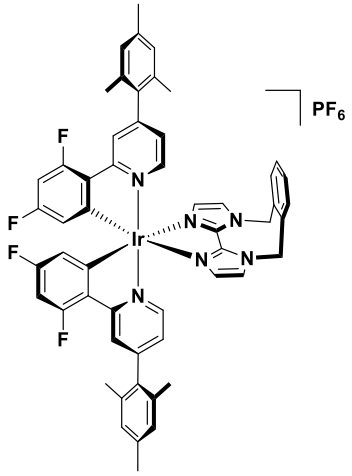

52

Figure **19**. Solubilised iridium complex bearing a substituted biimidazole ligand.

A complementary strategy for ancillary ligand design in the context of blue emission is to reduce the π-accepting strength of the ligand while maintaining the strong σ-donating character of the coordinating nitrogen atoms. One method to implement this strategy is to partially saturate the ligand scaffold while nevertheless maintaining sp^2-nitrogen coordinating atoms. One way in which this was done previously was by utilising bis-*N*-heterocyclic carbene (NHC) ligands, which are bridged by methylene groups such as complex **46**.[52a] These

ligands combine the exceptional σ-donating capabilities of NHCs with a lack of conjugation across the ligand scaffold, allowing these complexes to achieve very deep blue emission (λ_{PL} = 440 nm in MeCN for **46**).[53] As with the **49** – **52**, the ancillary bis-NHC ligand of **46** is non-chomophoric, with this complex showing highly structured LC emission.

For our strategy we used guanidylpyridine, gpy, (**53** and **54**) or guanidylpyrazine, gpz, (**55**) ancillary ligands, wherein one of the coordinating heterocyclic rings is partially saturated and thus reduces the conjugation length of the ligand.[54] In particular, complexes **53** and **54** were targeted to produce blue emission. Two important optoelectronic effects result from the incorporation of gpy onto the complex. Firstly, due to the saturation present in the guanidyl ring, the LUMO becomes localised largely on the C^N ligands (as indicated by DFT and CV), rather than on the N^N ligand as is observed for complexes such as **2** and **3**. Secondly, the strongly electron-releasing nature of the coordinating nitrogen atom of guanidyl ring acts to destabilise both the HOMO and the LUMO, but the greater destabilisation of the LUMO and also the triplet state results in a net blue-shifted emission. A comparison of the emission maxima in MeCN solution of **53** (λ_{PL} = 503 nm) with **2** (λ_{PL} = 585 nm) and **54** (λ_{PL} = 470, 498 nm) with **3** (λ_{PL} = 515 nm) brings the electronic effect of the gpy ligand into stark focus. By contrast to **53** and **54**, **55** displays strongly red-shifted and broad, mixed CT-type emission. DFT calculations point to a LUMO that is largely localized on the electron-poor pyrazine ring, resulting in both a much lower emission energy (λ_{PL} = 640 nm) and a very low Φ_{PL} of 0.2%.

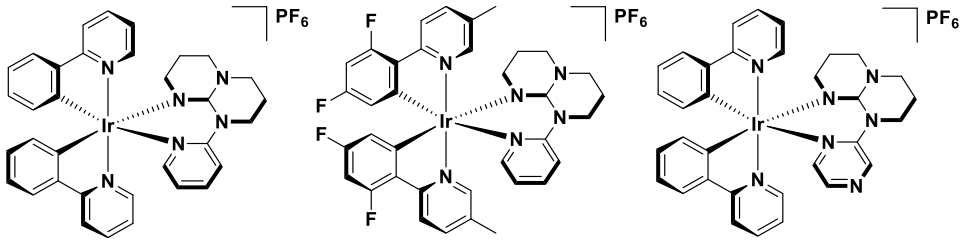

Figure **20**. Iridium complexes bearing guanidylpyridine (**53** and **54**) and guanidylpyrazine ancillary ligands (**55**).

Replacement of the coordinating nitrogen atoms for those that are at once more σ-donating and less π-accepting accomplishes the same effect. In particular, complexes bearing P^P ligands, such as **47**, have been explored in this vein.[55] Complex **47** is poorly emissive in MeCN solution (Φ_{PL} = 0.4%), but nevertheless is a deep blue emitter (λ_{PL} = 459 nm). We observed similar emission profiles when we explored a large family of complexes of the form $[Ir(ppy)_2(P\hat{}P)]PF_6$ where the bite angle of the P^P ligand was varied systematically (Figure **21**). In all cases, deep blue emission (λ_{PL} = 444 – 485 nm for the $E_{0\text{-}0}$ band in MeCN solution) was observed for the six ppy-containing complexes studied, regardless of the nature of the P^P ligand. However, each of these complexes also showed low Φ_{PL} values (Φ_{PL} = 0.3 – 4.2%).

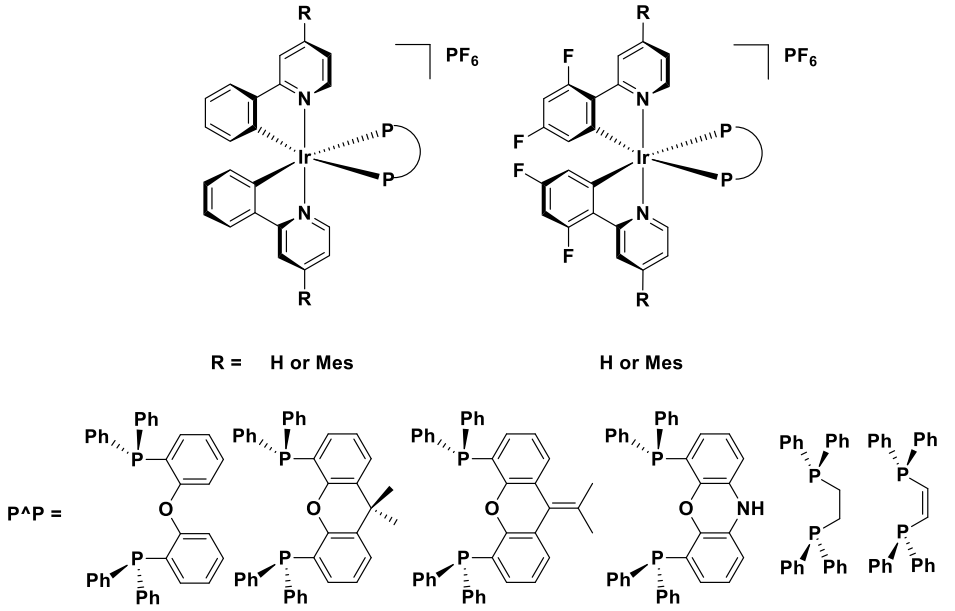

Figure **21**. General structures of iridium complexes explored with various P^P ancillary ligands.

By contrast, the nature of the C^N ligands impacted more greatly both the emission energy and, importantly, the Φ_{PL} of the complexes. When dFppy was employed as the C^N ligand (**56**), the expected blue-shift in the emission (λ_{PL} = 445 nm in MeCN for the $E_{0\text{-}0}$ band for **56** compared to 457 – 485 nm for the ppy complexes) was observed, and this coincided with a significant enhancement of the photoluminescence quantum yield (Φ_{PL} = 18%). Although this result is in line with the energy gap law, it is still nevertheless contradictory to what we would have expected, given that MC states should be more thermally accessible for **56** than for the other complexes.

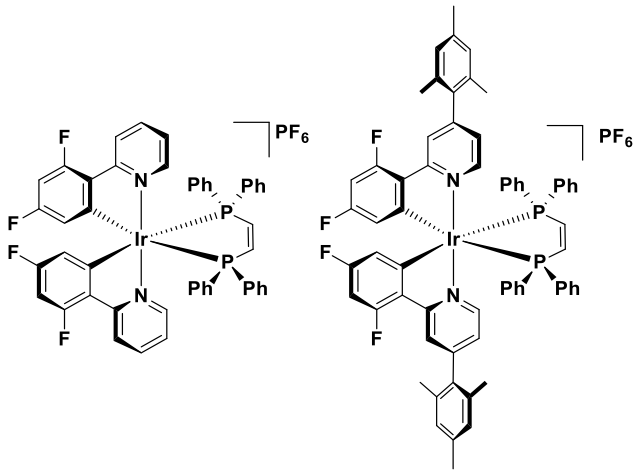

Figure **22**. Iridium complexes bearing P^P type ancillary ligands.

Accounting for the deep blue emission of all of these P^P complexes but their poor photoluminescence quantum yields led us to perform a substitution study to explore if we could maintain the deep blue colour but enhance the Φ_{PL} to appreciable levels. When studying the effects of the addition of a mesityl ring at the 4-position of the pyridine of the C^N ligands (2-phenyl-4-(2,4,6-trimethylphenyl)pyridine, Mesppy) we observed only an incremental enhancement of the Φ_{PL}. Similarly, when dFMesppy was used as the C^N ligand with wide bite-angle P^P ligands poorly emissive complexes were still observed (Φ_{PL} < 1.0%). However, combining dFMesppy with the smallest bite angle dppe ligand in **57** gratifyingly afforded both a bright and deep blue emission (λ_{PL} = 444 nm, Φ_{PL} = 52% in MeCN). When used in LEECs in a host-guest configuration, we found that **57** gave blue electroluminescence (λ_{EL} = 479 nm) but with low luminance (L_{max} = *ca* 7.5 cd m^{-2}) and poor stability ($t_{1/2}$ = 0.5 h). Such instability of bis-phosphine complexes in LEECs has been reported previously.[55b] We also targeted **57** for solution-processed OLEDs and showed that cationic iridium complexes could produce blue emission with CIE coordinates of (0.20, 0.29). However, despite the use of a mixed host-dopant configuration (host: mCP and OXD7) in the

emissive layer to improve charge balance, the efficiency was still low (EQE = 0.21%). Nevertheless, this example demonstrates the importance of optimising not only each ligand separately but also the combination of the ligands in order to achieve the desired properties of the complex. This point will be discussed further in Section 6.

Complex **55** illustrated the efficacy of incorporating within the ancillary ligand electron-withdrawing groups to red-shift the emission. Our study of complexes **58 – 61** combined this feature with increased conjugation across the ancillary ligand scaffold. The complexes possess an additional pyridine ring at the 5'-position of the N^N ligand. Two families were studied, with complexes **58** and **59** containing a 2,2':5',2''-terpyridine (2,5-tpy) ancillary ligand and **60** and **61** containing a 2,5-di(pyridin-2-yl)pyrazine (2,5-dpp) ancillary ligand. Comparison of the photophysics of **58** and **59** demonstrates the expected blue-shift of the emission as a function of the presence of the fluorine atoms on the C^N ligands, with the emission of **59** (λ_{PL} = 544 nm in MeCN) being blue-shifted compared to that of **58** (λ_{PL} = 605 nm in MeCN). Complex **59** is a very efficient emitter in solution (Φ_{PL} = 93%), particularly compared with **58** (Φ_{PL} = 6%). A comparison of the emission maxima of **58** and **1** (λ_{PL} = 602 nm in MeCN) suggests that the additional pyridine ring has a negligible effect on the electronics. However, the analogous comparison between **59** and **3** (λ_{PL} = 515 nm for **3** in MeCN) reveals a red-shift of the emission in the former compared to the latter.[11c]

By contrast, complexes **60** and **61**, containing the pyrazine ring, are significantly red-shifted in their emission compared to **58** and **59**. Despite containing dFMeppy C^N ligands, **61** shows essentially the same emission profile as **58** (λ_{PL} = 604 nm in MeCN for **61**), demonstrating that the nitrogen in the pyrazine ring is more influential to the photophysics than the extended conjugation, and that the inclusion of the pyrazine ring counterbalances the

HOMO-stabilizing effect of the fluorinated cyclometalating ligands. The emission in **60** is by far the most red-shifted of this family of complexes (λ_{PL} = 666 nm in MeCN), although it is also the least emissive (Φ_{PL} = 2.6%). This deep red emission translates to one of only four LEEC devices with CIE coordinates (CIE: 0.68, 0.33) that coincide with the ideal red coordinate. However, the lifetime of this device is short ($t_{1/2}$ = 6.3 h), and the efficiency is low (EQE = 0.08%),[11c] pointing towards the need for improved *molecular* and *device* design.

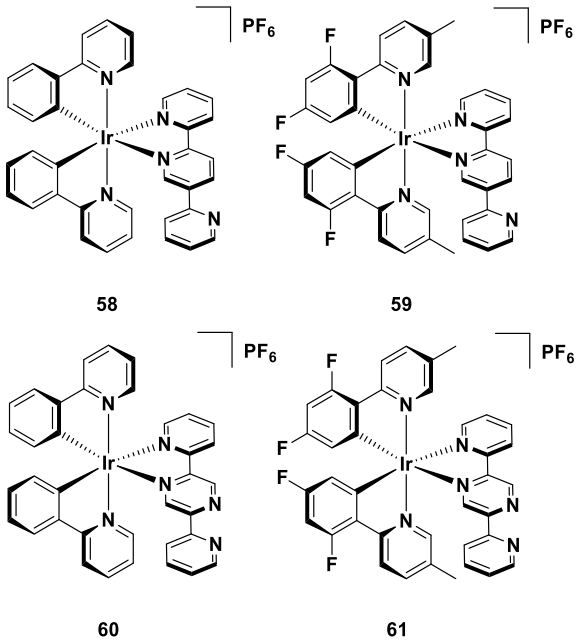

Figure **23**. Iridium complexes bearing 2,2':5',2''-terpyridine (**58** and **59**) or 2,5-di(pyridin-2-yl)pyrazine (**60** and **61**) as the ancillary ligand.

Another important aspect of these ancillary ligands is that they can function as bridging ligands. Previous work had shown that using 1,4-di(pyridine-2-yl)benzene as an ancillary ligand allowed the formation of neutral dinuclear iridium complexes.[56] In our efforts, we used the 2,5-dpp ligand as a bridging motif. It has been shown that adding multiple metals around a conjugated core can lead to a strong red-shift in the emission.[57] In this case, no emission could be detected at room temperature from the resultant dinuclear complex **62**, and thus it

was unclear if the emission had been too strongly red-shifted into the NIR, or if it was totally quenched. However, at 77 K in a 2-MeTHF glass emission from **62** (λ_{PL} = 715 nm) could be detected, and indeed this was greatly red-shifted compared to the emission of **60** under identical conditions (λ_{PL} = 589 nm at 77 K in 2-MeTHF glass).

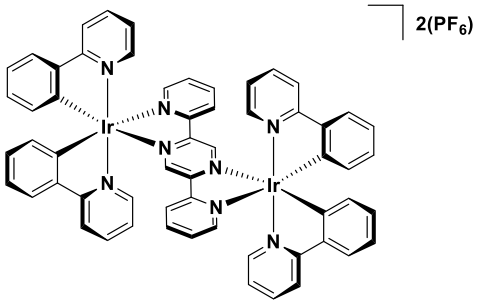

62

Figure **24**. Di-nuclear iridium complex bridged by 2,5-di(pyridin-2-yl)pyrazine.

A different strategy that we have employed for constructing bi- or multimetallic systems employs the 5-ethynyl-2,2'-bipyridine ligand, as with complexes **63** and **64**.[58] In 2-MeTHF solution the emission of both complexes **63** and **64** (λ_{PL} = 623 and 561 nm for **63** and **64**, respectively) is broad and unstructured, pointing towards typical ^{3}LLCT/^{3}MLCT emission. This emission is red-shifted compared to **1** and **3**, while also showing lower photoluminescence quantum yields (Φ_{PL} = 9% and 6% for **63** and **64**, respectively). The low Φ_{PL} values, particularly for **64**, were attributed to vibrations of the alkynyl group that provided a non-radiative decay outlet.

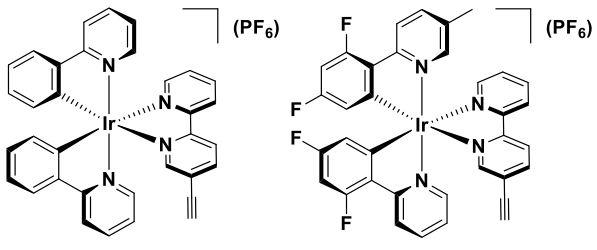

63 **64**

Figure **25**. Mono-nuclear iridium complexes bearing alkynyl substituents.

The dinuclear complexes were obtained by homocoupling **63** or **64** under Glaser conditions using CuCl. Comparing the corresponding dinuclear complexes **65** and **66**, we observed a surprising evolution in the photophysical properties. For complex **65**, the emission in 2-MeTHF showed the expected red-shift (λ_{PL} = 647 nm) in emission compared to the mononuclear parent with a corresponding decreased Φ_{PL} = 1%, pointing towards increased conjugation across the bipyridine ligand scaffold, and thus electronic communication between the two metal centres. However, to our surprise the dFMeppy analogues showed a different trend, with **66** somewhat *blue-shifted* (λ_{PL} = 558 nm) compared to its corresponding monomer, **64**. At 77 K, however, the expected pattern was indeed restored, with the monomeric complex **64** (λ_{PL} = 490, 527 nm at 77 K for **64**) undergoing a much more pronounced hypsochromic shift than its dimeric counterpart, **66** (λ_{PL} = 560, 605 nm at 77 K for **66**).

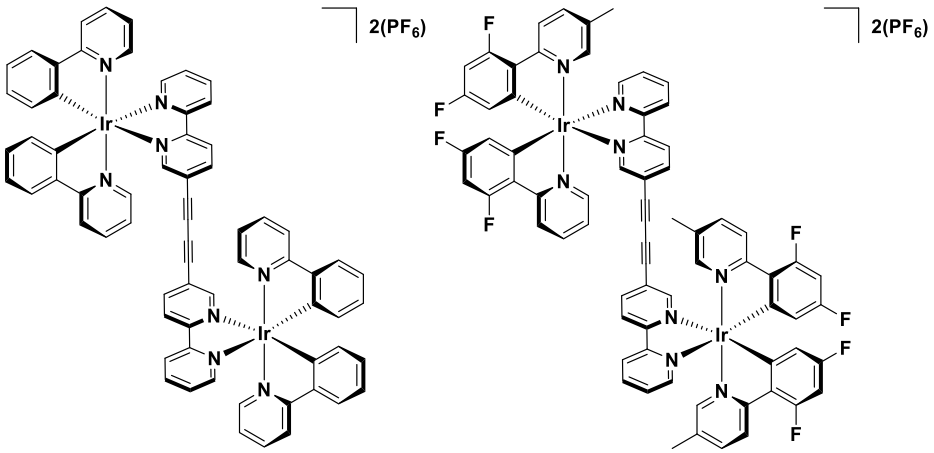

Figure **26**. Di-nuclear iridium complexes bearing alkynyl bridging units.

As we have seen, the mesityl substitution for complexes such as **3** and **52** can have a profound impact on the Φ_{PL} of the complex without impacting the emission energy. We[13a] investigated the effects on the optoelectronic properties of a series of complexes bearing diaryl-substituted bipyridine ligands (Figures **27** and **28**). Complexes **67** – **69** show modestly red-shifted emission compared to **1**, with **68** (λ_{PL} = 613 nm in MeCN) the bluest of these followed by **67** (λ_{PL} = 623 nm in MeCN) and **69** (λ_{PL} = 659 nm in MeCN). While **67** and **68** emit from a mixed CT state and are reasonably emissive (Φ_{PL} = 17% for **67** and Φ_{PL} = 21% for **68** compared to 6% for **1**), the strongly electron-donating character of the pendant dimethylamine groups in **69** forces a change in the excited state to that of an intraligand charge transfer (ILCT) state, with a correspondingly low Φ_{PL} of 0.7%. These results suggest that the strategy of incorporating steric bulk at the 5 and 5' positions of the bipyridine helps to enhance Φ_{PL} without modulating significantly the emission energy, assuming mixed CT emission is maintained, in an analogous fashion to the mesityl-substituted complexes discussed above. In addition, **67** is notable for its performance in a LEEC, which demonstrated greatly enhanced device stability under constant current driving compared to a control based on **2** ($t_{1/2}$ = 1.3 h for **2** and 110 h **67**).[59]

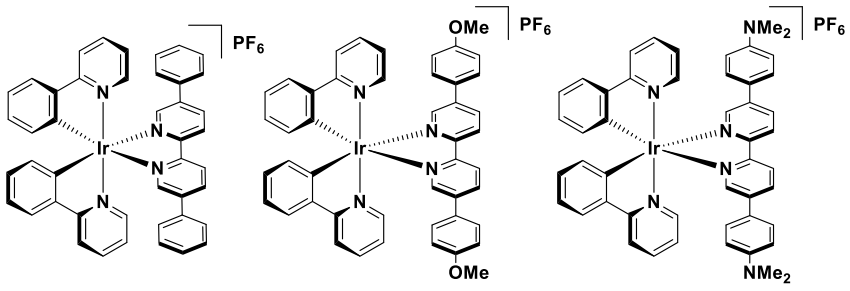

67 68 69

Figure **27**. Iridium complexes bearing diaryl substituted bipyridine ancillary ligands.

We explored the effects of decoupling mesomeric conjugation completely through the addition of *ortho,ortho*-dimethyl groups on the aryl substituents in **70** – **73**. Such a substitution resulted in a series of complexes with slightly blue-shifted emission maxima compared to **67** – **69** and **1** (λ_{PL} = 592 – 613 nm in MeCN) coupled with an enhancement in the Φ_{PL}. For example, complexes **70** (Φ_{PL} = 22%) and **71** (Φ_{PL} = 21%) are brighter than **67**, while **73** (Φ_{PL} = 2%) is also enhanced compared **69**.

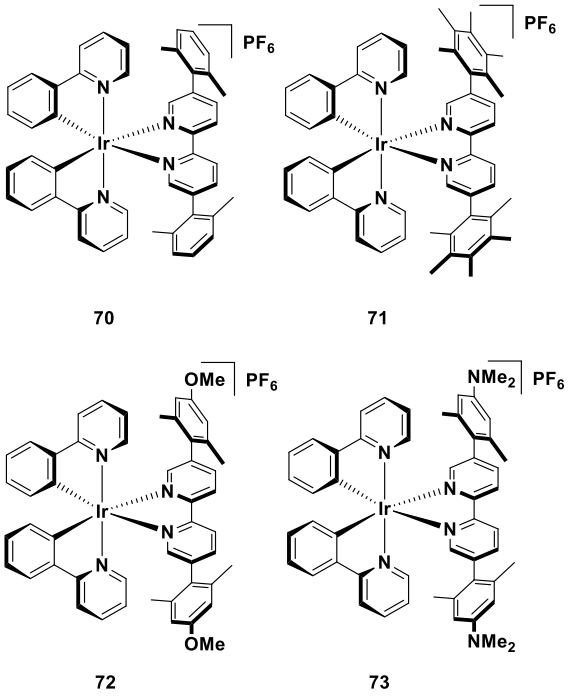

Figure **28**. Iridium complexes bearing bulky diaryl substituted bipyridine ancillary ligands.

Thus, we have seen examples of both deep blue and deep red emitters in solution. We have further illustrated examples of how careful molecular design can lead to *efficient* (blue) emitters in solution and demonstrated that incorporation of bulky groups inhibit intermolecular quenching processes that can reduce the Φ_{PL}. However, achieving a particular colour is now not enough. For blue emission, an important challenge that remains to be addressed is controlling the interplay between LC and CT states governing the emission. For device applications, CT states are typically preferred as the nature of these excited states

mean that they generally display shorter lifetimes (reduced triplet quenching) and narrower emission profiles (improved colour purity).[6c] However, as we have seen, maintaining a mixed CT triplet state becomes increasingly difficult as N^N ligands with higher orbital energies are employed. This behaviour in part accounts for the lack of a deep blue LEEC device reported to date. For red emission, although there are examples of 'true red' LEEC devices, these devices are invariably unstable, and poorly efficient. This is at least in part a consequence of the energy gap law, which negatively impacts the Φ_{PL} of the emitter.

6: C^N and N^N Ligand – Combining Substitution on Both Ligands

We have seen that modification of individual components of either the C^N or N^N ligands can modulate quite effectively the optoelectronic properties of the emitters. However, in order to optimize these properties it is frequently necessary to install both bespoke C^N and N^N ligands. Indeed, many of the examples presented from other groups such as **10**, **11** or **46** explore deviations both from the traditional C^N-type ligands (ppy and dFppy) and the conventional N^N ligand (bpy). We have also explored these strategies, primarily within the context of designing deep blue emitters, and frequently found that these structure-property relationship studies are not straightforward to interpret. As we observed with the red-emitting complexes **29a** – **32b**, there is a limit to how far we can tune the photophysics (in either the red or blue direction) of these cationic complexes by simple ligand substitution. This has so far precluded others and us from realising the goal of developing deep blue, highly emissive cationic iridium complexes functioning with good efficiency and stability in the device.

The first example of our efforts in this endeavour is based on complex **4**, originally reported by Nazeeruddin and co-workers.[60] This complex incorporates strongly electron-donating dimethylamino groups at the 4,4'-positions of the bipyridine ligands designed to

destabilise the LUMO and shift the emission to the blue. The blue-shifting capacity of this ancillary ligand is evidenced by comparing the emission of reference complexes **74** and **75** with that of **3**. Complexes **74** and **75** both show ^{3}LC-type emission characterised by high energy shoulders in the region of 460 nm as well as principal emission bands in the 490 nm regime (λ_{PL} = 464, 490 nm for **74** and 466, and 494 nm for **75** in MeCN) compared to the red-shifted ^{3}CT emission of **3** (λ_{PL} = 515 nm for **3** in MeCN).

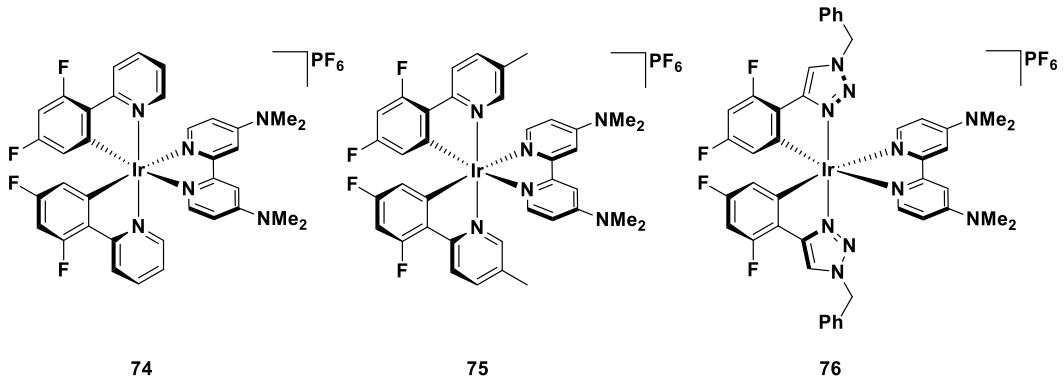

Figure **29**. Iridium complexes bearing 4,4'-dimethylamino-2,2'-bipyridine as the ancillary ligand.

In an effort to blue-shift this emission further, we incorporated the dFphtl ligand first reported coincidentally by De Cola and co-workers for **36** and **37**[41b] and by us for **41a** and **41b**[61] in order to take advantage of its blue-shifting properties relative to dFppy. However, to our surprise **76** exhibits sky-blue, unstructured emission (λ_{PL} = 495 nm in MeCN) that is essentially the same colour as **74** and **75**. To rationalize this result, we carried out DFT calculations to understand the effect of changing the ancillary ligand when the same dFphtl ligand was used (Figure **30**). Comparing **76** with **41a** and **41b**, we observed that the calculated energies of the HOMO orbitals were largely similar, with that of **76** slightly destabilised in comparison to the other two, as expected for substitution changes on the ancillary ligand. The LUMO energies increase with increased electron density on the N^N

ligands, leading to an overall increase in the band gap ($\Delta E_{HOMO\text{-}LUMO}$: **76** > **41b** > **41a**). Thus, on the basis of the band gaps calculated for the three complexes we would have expected the emission of **76** to be much bluer than both **41a** and **41b**, but this is not observed. Instead, DFT calculations reveal that the energy of the T_1 states for the three complexes remain essentially isoenergetic (modelled as the HSOMO energy in Figure **30**), indicating that the triplet energy is largely unaffected by the substitution of the -NMe_2 on the N^N ligand.

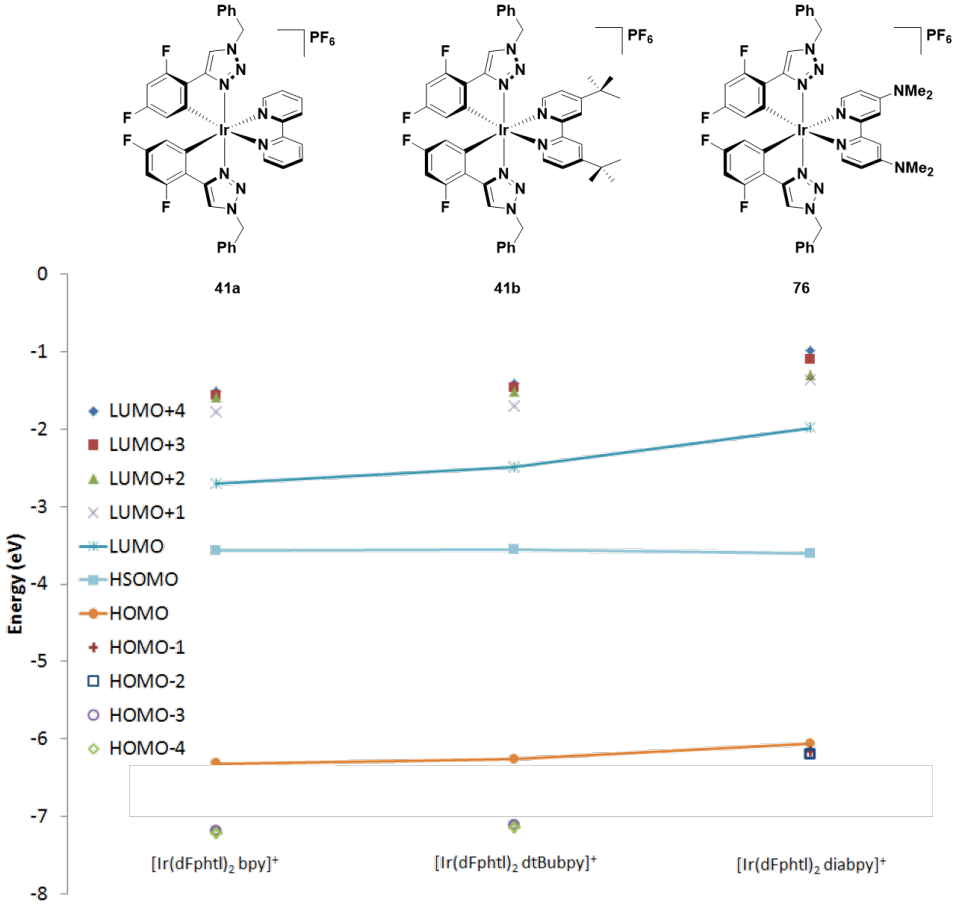

Figure **30**. DFT calculated energies of the HOMO-4 to LUMO+4 for complexes **41a**, **41b** and **76**, as well as the highest singly occupied molecular orbital (HSOMO) in the T_1 state. DFT [(B3LYP/SBKJC-VDZ for Ir(III)) and (6-31G* for C,H,N)] with CPCM (MeCN).

As the strategy of adding the most electron-donating substituent did not have the desired blue-shifting effect, we turned our attention to modifying the coordinating heterocycles of the

ancillary ligand. Complexes **77** and **78** employ the same bis-triazole ancillary ligand as in **48**.[49]

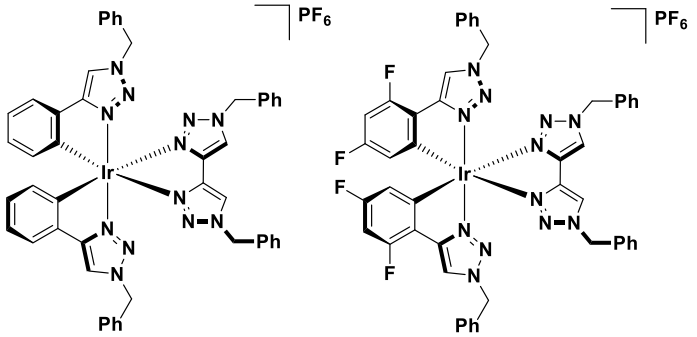

Figure **31**. Iridium complexes bearing 1,2,3-triazoles within the C^N and N^N ligand frameworks.

Comparing **48** and **77**, the emission of **77** is moderately bluer, showing ^{3}CT-type emission in the sky-blue region (λ_{PL} = 495 nm in MeCN), compared to the more structured ^{3}LC-type emission of **48** (λ_{PL} = 511 nm in MeCN with a high energy shoulder at 481 nm). This change in the nature of the emission is due to the capacity of the phtl ligand to increase the energy difference between the N^N-centred LUMO and C^N-centred LUMO+1 orbitals, thereby contributing to a more diffuse spin density distribution in the T_1 state and rendering the emission more CT-like. When fluorine atoms are incorporated on the C^N ligands in **78** we noticed that the complex becomes unusually photo-unstable, with the presence of two emission bands at room temperature at 352 nm and 505 nm, the latter of which diminished over time. LC-HRMS analysis of a photolysed sample showed that the primary degradation product was $[Ir(dFphtl)_2(NCMe)_2]^+$. These and ^{1}H NMR analyses pointed towards a photo-ejection of the btl ligand from the complex. Elliott and co-workers[62] independently corroborated this decomposition mechanism.

Despite the room temperature photoinstability of **78**, we were able to measure the emission of this complex at 77 K. Comparing the low temperature emission maxima of **78** with **77** and **48**, **78** is by far the bluest under these conditions (λ_{PL} = 470 nm for **78**, 407 nm for **77** and 393 nm for **78** in 2-MeTHF at 77 K), thus demonstrating the merits (from a colour tuning point of view) of 'optimising' the electronics of these complexes by addressing each individual ring.

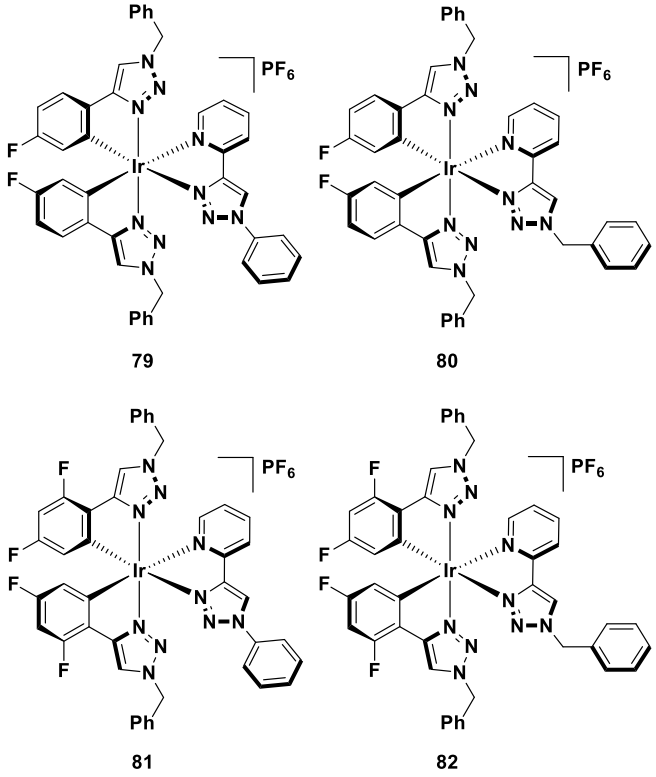

Figure **32**. Iridium complexes bearing pyridyltriazole ancillary ligands and Fphtl and dFphtl C^N ligands.

To establish a compromise between the blue-shifting qualities of the btl ligand with the associated photoinstability of its complexes, we synthesised complexes **79** – **82**, which contain pyridyltriazole ancillary ligands, similar to complex **43** and its analogues.[48] We explored two different pyridyltriazole ligands: one where the distal nitrogen was *N*-phenylated (**79** and **81**) and one where the distal nitrogen was *N*-benzylated (**80** and **82**). Each of these complexes employ either Fphtl or dFphtl as the C^N ligands, with only the number

of fluorine atoms appended to the phenyl ring being varied. As would be expected, the complexes where the phenyl ring has been substituted with only one fluorine atom (**79** and **80**) are not as blue in MeCN solution (λ_{PL} = 487 nm and 485 nm for **79** and **80**, respectively) than when there are two fluorine atoms present as in **81** and **82** (λ_{PL} = 461 nm and 452 nm for **81** and **82**, respectively). In addition, complexes **79** and **81**, where the phenyl rings are conjugated into the N^N ligand framework, are slightly red-shifted in emission compared to their *N*-benzyl substituted counterparts. Finally, complex **43** is in fact blue-shifted (λ_{PL} = 452, 483 nm) compared with complexes **79** – **82**, albeit with the caveat that the photophysics of **42** were investigated in DCM rather than MeCN for complexes **79** – **82**.

Although the Φ_{PL} of all the complexes were low (Φ_{PL} = 0.03 – 0.3% in MeCN), particularly compared to **43** (Φ_{PL} = 22%), the strongly blue-shifted emission of **81** and **82** in particular led us to explore the application of all four of these complexes as emitters in LEECs. Studying their properties in the solid state, we found that the neat film photophysics were similar to those in the solution state, with low Φ_{PL} values (Φ_{PL} = 1 – 2% for complexes **79** – **82**) but with strongly blue-shifted emission colour (λ_{PL} = 451 – 473 nm for complexes **79** – **82**); powder Φ_{PL} for **80** and **82** were however enhanced at 12 and 10%, respectively. Within the LEEC, we were surprised that the electroluminescence measurements were not consistent with the photoluminescence measurements. All of the complexes displayed red-shifted electroluminescence profile compared to their photoluminescence in both solution or the solid state. Furthermore, we observed that the trend in emission colour as a function of fluorine content of the C^N ligands had reversed: complexes **79** and **80**, which contained mono-fluorinated C^N ligands, in fact produced bluer emitting devices [λ_{EL} = 508 nm and 487 nm for **79** and **80** respectively; CIE: (0.31, 0.44) for **79** and (0.26, 0.36) for **80**] than the

difluorinated analogues [λ_{EL} = 569 nm and 508 nm for **81** and **82**, respectively; CIE: (0.37, 0.45) and (0.28, 0.45) for **81** and **82**]. Although this red-shift was undesired, the emission colour produced from the LEEC based on **80** is comparable to some of the best and bluest LEECs reported to date. In terms of CIE values, only a small number of iridium complexes have been reported to date that show bluer CIE coordinates in a LEEC. Complex **42** has the bluest CIE value reported to date (CIE: 0.20, 0.28),[9] while strongly blue-shifted emission is also observed from complex **33** (CIE: 0.20, 0.36),[39c] **83** (CIE: 0.21, 0.33)[63] and **84** (CIE: 0.20, 0.34).[53] Finally, although the CIE values for the LEEC with **43** and its analogues were not reported, the significantly bluer electroluminescence maxima reported for these complexes (λ_{EL} = 456 – 460 nm)[48] compared to **79** – **82** suggests that the CIE coordinates of these complexes are likely bluer in the device as well, despite these complexes bearing dFppy as the cyclometalating ligand, rather than dFphtl.

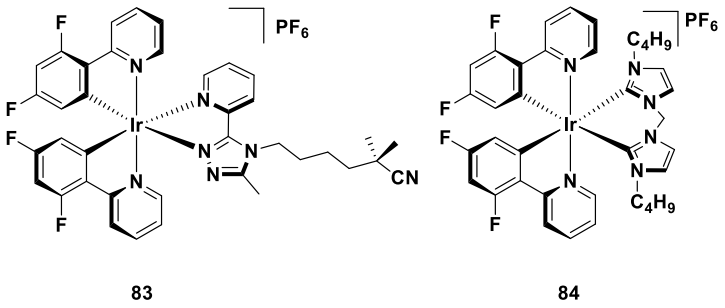

83 84

Figure **33**. Iridium complexes displaying blue emission in LEECs.

Given the very small change in photoluminescence properties in moving from solution to the solid state for all four of these complexes, the red-shift observed in the electroluminescence of complexes **79** – **82** is unlikely to be due to film morphology, assuming similar solution-processing protocols. As has been identified in the literature, there are normally two possible explanations for this kind of phenomenon: 1) the

electroluminescence mechanism gives rise to excimers, in which the effect is stronger for the difluorinated complexes **80** and **81**, or **2**) in the device there is a reordering of the relative energies of multiple emissive triplet states, which although close in energy *to each other*, may in fact differ significantly in their respective *emission energies*.[64] Regarding the first explanation, there are several reports of excimer formation in LEECs (such as complexes **85** and **86**), but frequently there is little to no characterisation of how such excimers form in the device, particularly given the pseudo-spherical nature of the Ir iTMC, making it difficult to assess the validity of this explanation.[37, 65] The second explanation has been invoked for **87**[64] and other complexes[66] where one of multiple different emissive triplet states (which differ significantly in their respective emission energies) are operative based on their environment. It is unclear which of these possibilities are operative in the case of complexes **79** – **82**, but these examples serve to illustrate the difficulty in translating the performance of these complexes in the solution state, all the way to the device.

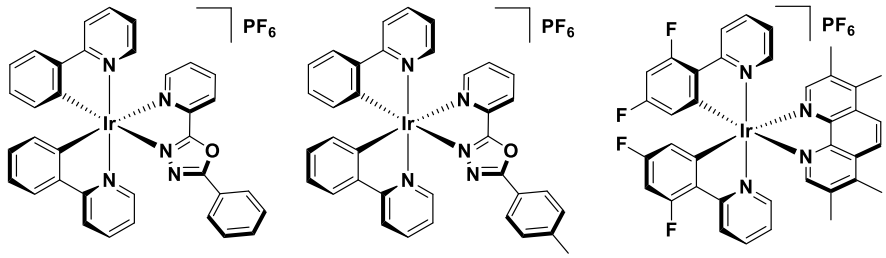

85 86 87

Figure **34**. Iridium complexes reported to display significant red-shift in their electroluminescence profiles. For complexes **85** and **86**, this was attributed to excimer formation,[37] while for **87** this was explained to be a result of reordering of multiple emissive states which are close in relative energy with respect to each other, but differ greatly in terms of their emission energies.[64]

In this section we have seen how unusual, unpredictable and 'non-linear' the evolution of the photophysical properties of these complexes can be when departing heavily from the

archetypal structures of complexes **1** and **2**. Complex **76** hit a 'photophysical wall' when blue-shifting emission; **78** was found to be photophysically unstable; complexes **79** and **80** were *bluer* than their analogues **81** and **82** in the solid state. Although we have been able to explain and rationalise the properties underpinning some of these complexes, they remain interesting examples that do not fit the traditional models.

Conclusions

Within this perspective article we have explored in a systematic fashion the evolution in photophysical properties of cationic iridium complexes as the C^N or N^N ligands are changed individually. We have also examined cases where modulation of the structure of both ligands works to tune the optoelectronic properties in concert. A combination of theoretical modelling, physical organic chemistry and knowledge of the prior art have proved to be useful tools in this endeavour. However, even with this confluence of knowledge and experience, we have found on more than one occasion that the properties of the bespoke complexes do not always fit the expected trends, illustrating the challenges faced when designing new materials. Even in instances when complexes behave in an expected way in one medium, such as in solution, their properties may not necessarily translate in a predictable fashion to other media such as thin films or in electroluminescent devices. A greater understanding of how the optoelectronic properties of these emitters change upon moving from the solution state to the solid state is certainly required in order to design improved emitters that produce EL devices with enhanced performance metrics. The breadth of examples illustrated herein should demonstrate unequivocally the potential of cationic iridium complexes and their use in optoelectronic applications.

Acknowledgements. EZ-C acknowledges past and present group members for their tireless efforts and enthusiasm and the University of St Andrews for financial support. We thank Johnson Matthey and Umicore AG for the gift of materials. We would like to thank the Engineering and Physical Sciences Research Council for financial support for Adam Henwood (EPSRC DTG Grants: EP/J500549/1; EP/K503162/1; EP/L505097/1).

References

(1). Y. You and W. Nam, *Chem. Soc. Rev.*, 2012, **41**, 7061-7084.
(2). (a) V. Guerchais and J.-L. Fillaut, *Coord. Chem. Rev.*, 2011, **255**, 2448-2457; (b) X. D. Wang and O. S. Wolfbeis, *Chem Soc Rev*, 2014, **43**, 3666-3761.
(3). (a) K. Lo, K. Tsang, K. Sze, C. Chung, T. Lee, K. Zhang, W. Hui, C. Li, J. Lau and D. Ng, *Coord. Chem. Rev.*, 2007, **251**, 2292-2310; (b) K. K.-W. Lo, M.-W. Louie and K. Y. Zhang, *Coord. Chem. Rev.*, 2010, **254**, 2603-2622; (c) K. K. Lo, *Acc Chem Res*, 2015, **48**, 2985-2995.
(4). (a) K. Teegardin, J. I. Day, J. Chan and J. Weaver, *Organic Process Research & Development*, 2016, **20**, 1156-1163; (b) C. K. Prier, D. A. Rankic and D. W. C. MacMillan, *Chem. Rev.*, 2013, **113**, 5322-5363.
(5). (a) Y. J. Yuan, Z. T. Yu, J. G. Cai, C. Zheng, W. Huang and Z. G. Zou, *ChemSusChem*, 2013, **6**, 1357-1365; (b) M. S. Lowry and S. Bernhard, *Chem. Eur. J.*, 2006, **12**, 7970-7977; (c) J. M. Thomsen, D. L. Huang, R. H. Crabtree and G. W. Brudvig, *Dalton Trans.*, 2015, **44**, 12452-12472.
(6). (a) For a recent review on iridium-based LEECs see: C. Ulbricht, B. Beyer, C. Friebe, A. Winter and U. S. Schubert, *Adv. Mater.*, 2009, **21**, 4418-4441. ; (b) H. Yersin, *Highly Efficient OLEDs with Phosphorescent Materials*, Wiley-VCH, Weinheim, 2008; (c) H. Yersin, A. F. Rausch, R. Czerwieniec, T. Hofbeck and T. Fischer, *Coord. Chem. Rev.*, 2011, **255**, 2622-2652.
(7). (a) R. D. Costa, E. Ortí, H. J. Bolink, F. Monti, G. Accorsi and N. Armaroli, *Angew. Chem. Int. Ed.*, 2012, **51**, 8178-8211; (b) A. F. Henwood and E. Zysman-Colman, *Top. Curr. Chem.*, 2016, **374**, 1-41; (c) J. D. Slinker, J. Rivnay, J. S. Moskowitz, J. B. Parker, S. Bernhard, H. D. Abruña and G. G. Malliaras, *J. Mater. Chem.*, 2007, **17**, 2976-2988.
(8). (a) For recent reviews see: L. Flamigni, A. Barbieri, C. Sabatini, B. Ventura and F. Barigelletti, *Top. Curr. Chem.*, 2007, **281**, 143-203. ; (b) K. P. S. Zanoni, R. L. Coppo, R. C. Amaral and N. Y. Murakami Iha, *Dalton Trans.*, 2015, **44**, 14559-14573; (c) Y. Chi and P.-T. Chou, *Chem. Soc. Rev.*, 2010, **39**, 638-655.
(9). L. He, L. Duan, J. Qiao, R. Wang, P. Wei, L. Wang and Y. Qiu, *Adv. Funct. Mater.*, 2008, **18**, 2123-2131.
(10). K. Shanmugasundaram, M. S. Subeesh, C. D. Sunesh and Y. Choe, *RSC Adv.*, 2016, **6**, 28912-28918.
(11). (a) For representative of white-emitting LEECs see: L. He, J. Qiao, L. Duan, G. Dong, D. Zhang, L. Wang and Y. Qiu, *Adv. Funct. Mater.*, WILEY-VCH Verlag, 2009, **19**, 2950-2960. ; (b) R. D. Costa, F. J. Cespedes-Guirao, E. Orti, H. J. Bolink, J. Gierschner, F.

Fernandez-Lazaro and A. Sastre-Santos, *Chem. Commun.*, 2009, 3886-3888; (c) K. Hasan, L. Donato, Y. Shen, J. D. Slinker and E. Zysman-Colman, *Dalton Trans.*, 2014, **43**, 13672-13682; (d) A. B. Tamayo, S. Garon, T. Sajoto, P. I. Djurovich, I. M. Tsyba, R. Bau and M. E. Thompson, *Inorg. Chem.*, 2005, **44**, 8723-8732.
(12). (a) M. G. Colombo and H. U. Güdel, *Inorg. Chem.*, 1993, **32**, 3081-3087; (b) M. G. Colombo, A. Hauser and H. U. Güdel, *Inorg. Chem.*, 1993, **32**, 3088-3092; (c) J. D. Slinker, A. A. Gorodetsky, M. S. Lowry, J. Wang, S. T. Parker, R. Rohl, S. Bernhard and G. G. Malliaras, *J. Am. Chem. Soc.*, 2004, **126**, 2763; (d) R. D. Costa, E. Ortì, H. J. Bolink, S. Graber, S. Schaffner, M. Neuburger, C. E. Housecroft and E. C. Constable, *Adv. Funct. Mater.*, 2009, **19**, 3456-3463; (e) R. D. Costa, E. Ortí, D. Tordera, A. Pertegás, H. J. Bolink, S. Graber, C. E. Housecroft, L. Sachno, M. Neuburger and E. C. Constable, *Adv. Energy Mater.*, 2011, **1**, 282-290.
(13). (a) S. Ladouceur, D. Fortin and E. Zysman-Colman, *Inorg. Chem.*, 2010, **49**, 5625-5641; (b) D. Tordera, M. Delgado, E. Ortí, H. J. Bolink, J. Frey, M. K. Nazeeruddin and E. Baranoff, *Chem. Mater.*, 2012, **24**, 1896-1903.
(14). S. Ladouceur and E. Zysman-Colman, *Eur. J. Inorg. Chem.*, 2013, **2013**, 2985-3007.
(15). (a) M. Bixon, J. Jortner, J. Cortes, H. Heitele and M. E. Michel-Beyerle, *J. Phys. Chem.*, 1994, **98**, 7289-7299; (b) J. V. Caspar and T. J. Meyer, *J. Phys. Chem.*, 1983, **87**, 952-957.
(16). A. F. Henwood, A. K. Bansal, D. B. Cordes, A. M. Z. Slawin, I. D. W. Samuel and E. Zysman-Colman, *J. Mater. Chem. C*, 2016, **4**, 3726-3737.
(17). H. J. Bolink, E. Coronado, R. n. D. Costa, N. Lardiés and E. Ortì, *Inorg. Chem.*, 2008, **47**, 9149-9151.
(18). V. N. Kozhevnikov, Y. Zheng, M. Clough, H. A. Al-Attar, G. C. Griffiths, K. Abdullah, S. Raisys, V. Jankus, M. R. Bryce and A. P. Monkman, *Chem. Mater.*, 2013, **25**, 2352-2358.
(19). A. K. Pal, D. B. Cordes, A. M. Z. Slawin, C. Momblona, E. Ortı´, I. D. W. Samuel, H. J. Bolink and E. Zysman-Colman, *Inorg. Chem.*, 2016, **55**, 10361-10376.
(20). J. Frey, B. F. E. Curchod, R. Scopelliti, I. Tavernelli, U. Rothlisberger, M. K. Nazeeruddin and E. Baranoff, *Dalton Trans.*, 2014, **43**, 5667-5679.
(21). X. Yang, X. Xu and G. Zhou, *J. Mater. Chem. C*, 2014, **3**, 913-944.
(22). N. M. Shavaleev, R. Scopelliti, M. Grätzel, M. K. Nazeeruddin, A. Pertegás, C. Roldán-Carmona, D. Tordera and H. J. Bolink, *J. Mater. Chem. C*, 2013, **1**, 2241.
(23). (a) C. D. Ertl, J. Cerdá, J. M. Junquera-Hernández, A. Pertegás, H. J. Bolink, E. C. Constable, M. Neuburger, E. Ortí and C. E. Housecroft, *RSC Adv.*, 2015, **5**, 42815-42827; (b) C. Fan, Y. Li, C. Yang, H. Wu, J. Qin and Y. Cao, *Chem. Mater.*, 2012, **24**, 4581-4587; (c) D. Tordera, A. M. Bünzli, A. Pertegás, J. M. Junquera-Hernández, E. C. Constable, J. A. Zampese, C. E. Housecroft, E. Ortí and H. J. Bolink, *Chem. Eur. J.*, 2013, **19**, 8597-8609.
(24). H. J. Bolink, L. Cappelli, E. Coronado, A. Parham and P. Stossel, *Chem. Mater.*, 2006, **18**, 2778-2780.
(25). J.-H. Lee, G. Sarada, C.-K. Moon, W. Cho, K.-H. Kim, Y. G. Park, J. Y. Lee, S.-H. Jin and J.-J. Kim, *Advanced Optical Materials*, 2015, **3**, 211-220.
(26). (a) S. J. Lee, K.-M. Park, K. Yang and Y. Kang, *Inorg. Chem.*, 2008, **48**, 1030-1037; (b) Y. Kang, Y.-L. Chang, J.-S. Lu, S.-B. Ko, Y. Rao, M. Varlan, Z.-H. Lu and S. Wang, *J. Mater. Chem. C*, 2013, **1**, 441-450; (c) H. Oh, K.-M. Park, H. Hwang, S. Oh, J. H. Lee, J.-S. Lu, S. Wang and Y. Kang, *Organometallics*, 2013, **32**, 6427-6436; (d) C.-H. Yang, M. Mauro, F. Polo, S. Watanabe, I. Muenster, R. Fröhlich and L. De Cola, *Chem. Mater.*, 2012, **24**, 3684-3695.
(27). (a) B. J. Coe, M. Helliwell, S. Sanchez, M. K. Peers and N. S. Scrutton, *Dalton Trans*, 2015, **44**, 15420-15423; (b) B. J. Coe, M. Helliwell, J. Raftery, S. Sanchez, M. K. Peers and N. S. Scrutton, *Dalton Trans*, 2015, **44**, 20392-20405.

(28). (a) C. H. Chang, Z. J. Wu, C. H. Chiu, Y. H. Liang, Y. S. Tsai, J. L. Liao, Y. Chi, H. Y. Hsieh, T. Y. Kuo, G. H. Lee, H. A. Pan, P. T. Chou, J. S. Lin and M. R. Tseng, *ACS Appl. Mater. Interfaces*, 2013, **5**, 7341-7351; (b) T. Duan, T. K. Chang, Y. Chi, J. Y. Wang, Z. N. Chen, W. Y. Hung, C. H. Chen and G. H. Lee, *Dalton Trans*, 2015, **44**, 14613-14624.
(29). (a) V. Sivasubramaniam, F. Brodkorb, S. Hanning, H. P. Loebl, V. van Elsbergen, H. Boerner, U. Scherf and M. Kreyenschmidt, *J. Fluorine Chem.*, 2009, **130**, 640-649; (b) Y. Zheng, A. S. Batsanov, R. M. Edkins, A. Beeby and M. R. Bryce, *Inorg Chem*, 2012, **51**, 290-297; (c) D. Tordera, J. J. Serrano-Pérez, A. Pertegás, E. Ortí, H. J. Bolink, E. Baranoff, M. K. Nazeeruddin and J. Frey, *Chem. Mater.*, 2013, **25**, 3391-3397.
(30). (a) S. Altomonte and M. Zanda, *J. Fluorine Chem.*, 2012, **143**, 57-93; (b) P. R. Savoie and J. T. Welch, *Chem. Rev.*, 2014, **115**, 1130-1190.
(31). N. M. Shavaleev, G. Xie, S. Varghese, D. B. Cordes, A. M. Z. Slawin, C. Momblona, E. Ortí, H. J. Bolink, I. D. W. Samuel and E. Zysman-Colman, *Inorg. Chem.*, 2015, **54**, 5907-5914.
(32). J.-L. Bredas, *Materials Horizons*, 2014, **1**, 17.
(33). S. Evariste, M. Sandroni, T. W. Rees, C. Roldan-Carmona, L. Gil-Escrig, H. J. Bolink, E. Baranoff and E. Zysman-Colman, *J. Mater. Chem. C*, 2014, **2**, 5793-5804.
(34). K. Dedeian, P. I. Djurovich, F. O. Garces, G. Carlson and R. J. Watts, *Inorg. Chem.*, 1991, **30**, 1685-1687.
(35). D. L. Davies, M. P. Lowe, K. S. Ryder, K. Singh and S. Singh, *Dalton Trans.*, 2011, **40**, 1028-1030.
(36). K. Hasan, A. K. Bansal, I. D. W. Samuel, C. Roldán-Carmona, H. J. Bolink and E. Zysman-Colman, *Scientific Reports*, 2015, **5**, 12325.
(37). J. Zhang, L. Zhou, H. A. Al-Attar, K. Shao, L. Wang, D. Zhu, Z. Su, M. R. Bryce and A. P. Monkman, *Adv. Funct. Mater.*, 2013, **23**, 4667-4677.
(38). (a) J. L. Rodriguez-Redondo, R. D. Costa, E. Orti, A. Sastre-Santos, H. J. Bolink and F. Fernandez-Lazaro, *Dalton Trans.*, 2009, 9787-9793; (b) S. Graber, K. Doyle, M. Neuburger, C. E. Housecroft, E. C. Constable, R. n. D. Costa, E. Ortiz, D. Repetto and H. J. Bolink, *J. Am. Chem. Soc.*, 2008, **130**, 14944-14945.
(39). (a) C. D. Sunesh, G. Mathai, Y.-R. Cho and Y. Choe, *Polyhedron*, 2013, **57**, 77-82; (b) C. D. Sunesh, M. Chandran, G. Mathai and Y. Choe, *Opt. Mater.*, 2013, **35**, 407-413; (c) H.-B. Wu, H.-F. Chen, C.-T. Liao, H.-C. Su and K.-T. Wong, *Org. Electron.*, 2012, **13**, 483-490.
(40). H. J. Bolink, F. De Angelis, E. Baranoff, C. Klein, S. Fantacci, E. Coronado, M. Sessolo, K. Kalyanasundaram, M. Gratzel and M. K. Nazeeruddin, *Chem. Commun.*, 2009, 4672-4674.
(41). (a) B. Beyer, C. Ulbricht, D. Escudero, C. Friebe, A. Winter, L. González and U. S. Schubert, *Organometallics*, 2009, **28**, 5478-5488; (b) J. M. Fernández-Hernández, C.-H. Yang, J. I. Beltrán, V. Lemaur, F. Polo, R. Frõhlich, J. Cornil and L. De Cola, *J. Am. Chem. Soc.*, 2011, **133**, 10543–10558.
(42). (a) S.-C. Lo, C. P. Shipley, R. N. Bera, R. E. Harding, A. R. Cowley, P. L. Burn and I. D. W. Samuel, *Chem. Mater.*, 2006, **18**, 5119-5129; (b) C.-H. Yang, S.-W. Li, Y. Chi, Y.-M. Cheng, Y.-S. Yeh, P.-T. Chou, G.-H. Lee, C.-H. Wang and C.-F. Shu, *Inorg. Chem.*, 2005, **44**, 7770-7780.
(43). F. Monti, A. Baschieri, I. Gualandi, J. J. Serrano-Perez, J. M. Junquera-Hernandez, D. Tonelli, A. Mazzanti, S. Muzzioli, S. Stagni, C. Roldan-Carmona, A. Pertegas, H. J. Bolink, E. Orti, L. Sambri and N. Armaroli, *Inorg Chem*, 2014, **53**, 7709-7721.
(44). P. Pla, J. M. Junquera-Hernandez, H. J. Bolink and E. Orti, *Dalton Trans.*, 2015, **44**, 8497-8505.
(45). For examples see: S. Ladouceur, D. Fortin and E. Zysman-Colman, *Inorg. Chem.*, 2011, **50**, 11514-11526.

(46). V. V. Pavlishchuk and A. W. Addison, *Inorg. Chim. Acta*, 2000, **298**, 97-102.
(47). C. M. Cardona, W. Li, A. E. Kaifer, D. Stockdale and G. C. Bazan, *Adv. Mater.*, 2011, **23**, 2367-2371.
(48). M. Mydlak, C. Bizzarri, D. Hartmann, W. Sarfert, G. Schmid and L. De Cola, *Adv. Funct. Mater.*, 2010, **20**, 1812-1820.
(49). L. Donato, P. Abel and E. Zysman-Colman, *Dalton Trans.*, 2013, **42**, 8402-8412.
(50). N.-R. Jung, E.-J. Lee, J.-H. Kim, H.-K. Park, K.-M. Park and Y.-J. Kang, *Bull. Korean Chem. Soc.*, 2012, **33**, 183-188.
(51). A. F. Henwood, S. Evariste, A. M. Z. Slawin and E. Zysman-Colman, *Faraday Discuss.*, 2014, **174**, 165-182.
(52). (a) S. B. Meier, W. Sarfert, J. M. Junquera-Hernández, M. Delgado, D. Tordera, E. Ortí, H. J. Bolink, F. Kessler, R. Scopelliti, M. Grätzel, M. K. Nazeeruddin and E. Baranoff, *J. Mater. Chem. C*, 2013, **1**, 58; (b) J. M. Fernandez-Hernandez, S. Ladouceur, Y. Shen, A. Iordache, X. Wang, L. Donato, S. Gallagher-Duval, M. de Anda Villa, J. D. Slinker, L. De Cola and E. Zysman-Colman, *J. Mater. Chem. C*, 2013, **1**, 7440-7452; (c) C. D. Sunesh, K. Shanmugasundaram, M. S. Subeesh, R. K. Chitumalla, J. Jang and Y. Choe, *ACS Appl Mater Interfaces*, 2015, **7**, 7741-7751.
(53). C.-H. Yang, J. Beltran, V. Lemaur, J. Cornil, D. Hartmann, W. Sarfert, R. Fröhlich, C. Bizzarri and L. De Cola, *Inorg. Chem.*, 2010, **49**, 9891-9901.
(54). K. Hasan, A. K. Pal, T. Auvray, E. Zysman-Colman and G. S. Hanan, *Chem. Commun.*, 2015, **51**, 14060-14063.
(55). (a) M. S. Lowry, W. R. Hudson, R. A. Pascal Jr. and S. Bernhard, *J. Am. Chem. Soc.*, 2004, **126**, 14129-14135; (b) E. C. Constable, C. E. Housecroft, E. Schönhofer, J. Schönle and J. A. Zampese, *Polyhedron*, 2012, **35**, 154-160; (c) S.-X. Luo, L. Wei, X.-H. Zhang, M. H. Lim, K. X. V. Lin, M. H. V. Yeo, W.-H. Zhang, Z.-P. Liu, D. J. Young and T. S. A. Hor, *Organometallics*, 2013, **32**, 2908-2917.
(56). A. Tsuboyama, T. Takiguchi, S. Okada, M. Osawa, M. Hoshino and K. Ueno, *Dalton Trans.*, 2004, 1115-1116.
(57). (a) S. Culham, P. H. Lanoe, V. L. Whittle, M. C. Durrant, J. A. Williams and V. N. Kozhevnikov, *Inorg Chem*, 2013, **52**, 10992-11003; (b) V. N. Kozhevnikov, M. C. Durrant and J. A. G. Williams, *Inorg. Chem.*, 2011, **50**, 6304-6313.
(58). A. M. Soliman, D. Fortin, P. D. Harvey and E. Zysman-Colman, *Dalton Trans.*, 2012, **41**, 9382-9393.
(59). L. Sun, A. Galan, S. Ladouceur, J. D. Slinker and E. Zysman-Colman, *J. Mater. Chem.*, 2011, **21**, 18083-18088.
(60). (a) M. K. Nazeeruddin, R. T. Wegh, Z. Zhou, C. Klein, Q. Wang, F. DeAngelis, S. Fantacci and M. Grätzel, *Inorg. Chem.*, 2006, **45**, 9245-9250; (b) F. De Angelis, S. Fantacci, N. Evans, C. Klein, S. M. Zakeeruddin, J.-E. Moser, K. Kalyanasundaram, H. J. Bolink, M. Gratzel and M. K. Nazeeruddin, *Inorg. Chem.*, 2007, **46**, 5989-6001.
(61). (a) K. N. Swanick, S. Ladouceur, E. Zysman-Colman and Z. Ding, *Angew. Chemie. Int. Ed.*, 2012, **51**, 11079-11082; (b) S. Ladouceur, K. N. Swanick, S. Gallagher-Duval, Z. Ding and E. Zysman-Colman, *Eur. J. Inorg. Chem.*, 2013, **2013**, 5329-5343.
(62). C. E. Welby, G. K. Armitage, H. Bartley, A. Sinopoli, B. S. Uppal and P. I. Elliott, *Photochem Photobiol Sci*, 2014, **13**, 735-738.
(63). B. Chen, Y. Li, W. Yang, W. Luo and H. Wu, *Org. Electron.*, 2011, **12**, 766-773.
(64). H. J. Bolink, L. Cappelli, S. Cheylan, E. Coronado, R. D. Costa, N. Lardies, M. K. Nazeeruddin and E. Orti, *J. Mater. Chem.*, 2007, **17**, 5032-5041.
(65). E. C. Constable, C. E. Housecroft, G. E. Schneider, J. A. Zampese, H. J. Bolink, A. Pertegas and C. Roldan-Carmona, *Dalton Trans.*, 2014, **43**, 4653-4667.

(66). Z. Wang, L. He, L. Duan, J. Yan, R. Tang, C. Pan and X. Song, *Dalton Trans*., 2015, **44**, 15914-15923.

TOC Graphic: